Alaska Department of Transportation & Public Facilities

Alaska University Transportation Center

Impacts of Climate Variability and Change on Flood Frequency Analysis for Transportation Design

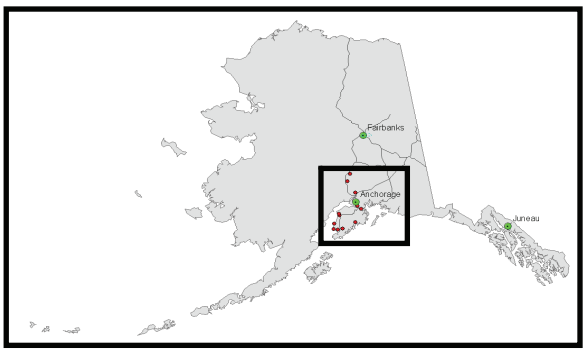

Prepared By:
Dr. Amy Tidwell

September 2010

Prepared For:

Alaska University Transportation Center
Duckering Building Room 245
P.O. Box 755900
Fairbanks, AK 99775-5900

Alaska Department of Transportation
Research, Development, and Technology Transfer
2301 Peger Road
Fairbanks, AK 99709-5399

INE # 11.02

FHWA-AK-RD-10-09

REPORT DOCUMENTATION PAGE

Form approved OMB No.

1. AGENCY USE ONLY (LEAVE BLANK)	2. REPORT DATE	3. REPORT TYPE AND DATES COVERED
FHWA-AK-RD-10-09	September 2010	Final Report

4. TITLE AND SUBTITLE
Impacts of Climate Variability and Change on Flood Frequency Analysis for Transportation Design

5. FUNDING NUMBERS
AUTC #207120
T2-08-17
DTRT06-G-0011

6. AUTHOR(S)
Dr. Amy Tidwell

7. PERFORMING ORGANIZATION NAME(S) AND ADDRESS(ES)
Alaska University Transportation Center
P.O. Box 755900
Fairbanks, AK 99775-5900

8. PERFORMING ORGANIZATION REPORT NUMBER
INE/AUTC 11.02

9. SPONSORING/MONITORING AGENCY NAME(S) AND ADDRESS(ES)
Alaska Department of Transportation
Research, Development, and Technology Transfer
2301 Peger Road
Fairbanks, AK 99709-5399

10. SPONSORING/MONITORING AGENCY REPORT NUMBER
FHWA-AK-RD-10-09

11. SUPPLENMENTARY NOTES

12a. DISTRIBUTION / AVAILABILITY STATEMENT
No restrictions

12b. DISTRIBUTION CODE

13. ABSTRACT (Maximum 200 words)

Planning for construction of roads and bridges over rivers or floodplains includes a hydrologic analysis of rainfall amount and intensity for a defined period. Infrastructure design must be based on accurate rainfall estimates — how much (intensity), how long (duration), and how often (frequency or probability). UAF and the National Oceanic and Atmospheric Administration are updating this important design tool with support from AUTC and ADOT&PF. Measuring precipitation in an environment like Alaska's is difficult. Challenges include poor gauge performance in windy environments, especially for solid precipitation (such as snow, sleet, and hail); and accessing and working in remote, sparsely populated, rough, and complex terrain. Another issue is the sparseness and distribution of the gauge stations. For example, the area north of the Brooks Range, known as the Arctic Slope of Alaska, is one of the least-understood climatic regions of the country. This region, with an area of over 230,000 square kilometers, has only a handful of long-term precipitation gauges, and many of the existing gauges are unattended. The quality of reported precipitation data varies due to gauge location, type, and whether or not a rain or snow gauge shield is present.

14- KEYWORDS: Hydrology, Precipitation, Rainfall, Floods, Streamflow

15. NUMBER OF PAGES
38

16. PRICE CODE
N/A

17. SECURITY CLASSIFICATION OF REPORT	18. SECURITY CLASSIFICATION OF THIS PAGE	19. SECURITY CLASSIFICATION OF ABSTRACT	20. LIMITATION OF ABSTRACT
Unclassified	Unclassified	Unclassified	N/A

SI* (MODERN METRIC) CONVERSION FACTORS

APPROXIMATE CONVERSIONS TO SI UNITS

Symbol	When You Know	Multiply By	To Find	Symbol
		LENGTH		
in	inches	25.4	millimeters	mm
ft	feet	0.305	meters	m
yd	yards	0.914	meters	m
mi	miles	1.61	kilometers	km
		AREA		
in^2	square inches	645.2	square millimeters	mm^2
ft^2	square feet	0.093	square meters	m^2
yd^2	square yard	0.836	square meters	m^2
ac	acres	0.405	hectares	ha
mi^2	square miles	2.59	square kilometers	km^2
		VOLUME		
fl oz	fluid ounces	29.57	milliliters	mL
gal	gallons	3.785	liters	L
ft^3	cubic feet	0.028	cubic meters	m^3
yd^3	cubic yards	0.765	cubic meters	m^3
	NOTE: volumes greater than 1000 L shall be shown in m^3			
		MASS		
oz	ounces	28.35	grams	g
lb	pounds	0.454	kilograms	kg
T	short tons (2000 lb)	0.907	megagrams (or "metric ton")	Mg (or "t")
		TEMPERATURE (exact degrees)		
^oF	Fahrenheit	5 (F-32)/9 or (F-32)/1.8	Celsius	^oC
		ILLUMINATION		
fc	foot-candles	10.76	lux	lx
fl	foot-Lamberts	3.426	$candela/m^2$	cd/m^2
		FORCE and PRESSURE or STRESS		
lbf	poundforce	4.45	newtons	N
lbf/in^2	poundforce per square inch	6.89	kilopascals	kPa

APPROXIMATE CONVERSIONS FROM SI UNITS

Symbol	When You Know	Multiply By	To Find	Symbol
		LENGTH		
mm	millimeters	0.039	inches	in
m	meters	3.28	feet	ft
m	meters	1.09	yards	yd
km	kilometers	0.621	miles	mi
		AREA		
mm^2	square millimeters	0.0016	square inches	in^2
m^2	square meters	10.764	square feet	ft^2
m^2	square meters	1.195	square yards	yd^2
ha	hectares	2.47	acres	ac
km^2	square kilometers	0.386	square miles	mi^2
		VOLUME		
mL	milliliters	0.034	fluid ounces	fl oz
L	liters	0.264	gallons	gal
m^3	cubic meters	35.314	cubic feet	ft^3
m^3	cubic meters	1.307	cubic yards	yd^3
		MASS		
g	grams	0.035	ounces	oz
kg	kilograms	2.202	pounds	lb
Mg (or "t")	megagrams (or "metric ton")	1.103	short tons (2000 lb)	T
		TEMPERATURE (exact degrees)		
^oC	Celsius	1.8C+32	Fahrenheit	^oF
		ILLUMINATION		
lx	lux	0.0929	foot-candles	fc
cd/m^2	$candela/m^2$	0.2919	foot-Lamberts	fl
		FORCE and PRESSURE or STRESS		
N	newtons	0.225	poundforce	lbf
kPa	kilopascals	0.145	poundforce per square inch	lbf/in^2

*SI is the symbol for the International System of Units. Appropriate rounding should be made to comply with Section 4 of ASTM E380.
(Revised March 2003)

Table of Contents

List of Figures

List of Tables

Acknowledgments

This research was funded jointly by the Alaska Department of Transportation and Public Facilities and the Alaska University Transportation Center. The author would also like to thank the staff of the USGS Alaska Science Center for assisting with data acquisition and being available to discuss technical aspects of the flood frequency analysis.

Chapter 1. Introduction and Problem Statement

Infrastructure designs, such as roads and bridges, require estimates of flood frequency and magnitude to adequately manage risk and balance construction, maintenance, and flood damage costs. Alarming trends in temperature and the potential for redistribution of fresh water has understandably led to concerns regarding changes in hydrology and the infrastructure affected by water. Although some projections suggest that significant climate change may occur over the same scales as the design life of roads, bridges, and water management projects, engineering design criteria continue to rely heavily on the assumption that historical conditions will persist into the future. Recent climate change documentation, as well as the importance of climate variability, seriously undermines the validity of this assumption.

Recent observations have led to concerns that peak flow statistics being used for design purposes in south-central Alaska may not be adequately characterizing the system behavior. In the past few decades, and particularly in the past several years, south-central Alaska has experienced noticeably high incidence of low probability flood events. For example, in 2002 the Kenai Peninsula experienced two months (October and November) of extreme flooding with estimated return periods greater than 100 years. The Trapper Creek area has experienced two flood events (1986 and 2006) with return periods in excess of 150-200 years within a 20 year period. On Montana Creek, 2 out of 12 years have experienced floods with greater than 100-year return periods, while Willow Creek has seen 2 out of 20 years. The public risk and infrastructure maintenance costs associated with the perceived higher than expected flood frequency suggests that there may be benefits to better understanding the regional hydrology.

If there is an underlying trend in the annual flood maxima, which form the basis for flood frequency analysis, then the estimated return periods for specified flows will eventually exhibit bias. This may lead to one of two outcomes: increased construction costs for over-designed structures under scenarios of decreasing flood frequency, or increased flood risk and damage for under-designed structures due to increasing flood frequency. Quantifying uncertainty provides a logical basis for minimizing the added risk associated with model errors, and evaluating the potential impacts of climate trends will aide an assessment of changing risk to the public.

The objective of this work was to determine if a climate trend and/or large scale climate variability may be causing significant biases in flood frequency estimates for Southcentral Alaska as well as the limits of detection for potential trends. Additionally, this work related uncertainty in flood frequency estimates to flood damage risk and developed a recommendation for better utilizing uncertainty estimates for selecting flood-based design criteria.

2: Methods

This research has employed a variety of analytic and numeric statistical techniques to address the underlying study questions. In the case of estimating annual flood frequencies, the techniques prescribed in Bulletin 17B (1982), produced by the Interagency Advisory Committee on Water Data (IACWD), have been implemented through the use of the USGS program PeakFQ (Flynn et al., 2006). Bulletin 17B was developed for use by federal, state and other public entities for flood frequency applications.

Two numerical techniques were used in conjunction with the standard flood frequency estimation: the bootstrap and Monte Carlo simulation. The bootstrap (Efron, 1982; Efron and Tibshirani, 1993) is a resampling technique used in statistical inference. The ordinary bootstrap is a non-parametric approach and does not depend on underlying distribution assumptions. Resampling occurs from a set of observed data- in this case, historical peak annual flow data- and uses the empirical distribution in place of an assumed statistical model. Monte Carlo simulation involves repeated random sampling from a specified analytical distribution. The primary differences between Monte Carlo and bootstrapping are 1) Monte Carlo uses a prescribed probability distribution rather than an empirical distribution, and 2) bootstrapped samples are limited by the original observed sample, while Monte Carlo is not necessarily constrained to sample from a finite set. Both techniques are powerful tools for evaluating distributional properties of complex statistics.

Finally, the non-parametric Mann-Kendall test for trend has been applied to annual maximum flow series. As discussed later, this test is applied directly to the annual maximum time series of data and does not employ distribution fitting as with the split-sample tests used in conjunction with flood quantile estimates.

The following sections describe the specific analyses conducted in this research and how the aforementioned statistical techniques have been used. The analyses have been broken down as follows: 1) Split sample tests for changes in flood quantiles; 2) Test for trends in magnitude and timing of annual maximum flow; 3) Detection limits for known trends; and 4) Confidence intervals for flood risk. Results and discussion will be addressed in the same order later in the report.

2.1 Split sample tests for changes in flood quantiles

Twelve stream gauging sites in Southcentral Alaska (see Site Selection below) were evaluated for evidence of climate trend or climate variability effects in flood frequency estimates. The historical peak annual flow data at each site were split into two samples in order to evaluate possible changes in flood quantiles, such as the 2-year or 100-year flood, between two periods in time. The following statistical hypothesis was tested using the previously mentioned bootstrapping technique:

Null Hypothesis (Ho): Flood quantiles (flood frequency estimates) have no time-dependent trend.

Alternate Hypothesis (Ha): Flood quantiles are changing over time.

Under *Ho*, peak annual flow data from both samples were considered to be from the same underlying population. Therefore, the distribution of the differences between each of the flow quantiles (e.g., Q_2 or Q_{100}) should have a mean near zero, but an otherwise unknown distribution. The bootstrap was used to generate the null distribution for the differences between Sample 1 (S1) and Sample 2 (S2), where S1 represented the first *n1* years of record and S2 represented the last *n2* years of record. 2000 replicates of samples 1 and 2, with samples sizes *n1* and *n2*, were drawn with replacement from the pooled period of record ($n = n1 + n2$) in accordance with *Ho*. Each replicate was then used with the USGS program PeakFQ to estimate the flood distribution and specific quantiles. The result was an empirical null distribution of S1-S2 for each flood quantile of interest. Finally, the actual values of S1-S2 were compared with the null distribution to determine if the differences were significantly different than zero in light of the underlying variability of the null distribution.

The split-sample analysis was setup in two different ways. First, the historical record at each station was split simply according to early years (< 1981) versus late years (>1980) to evaluate the possible existence of an underlying climate trend. Second, the record was split according to the modes of the Pacific Decadal Oscillation (PDO), with PDO- occurring from 1947-1976 and PDO+ occurring from 1977-1998 (Mantua et al., 1997).

2.2 Test for trends in magnitude and timing of annual maximum flow

In the previous analysis, peak annual flows were used together with PeakFQ to estimate the flood distribution and specific flood quantiles. In this analysis, the non-parametric Mann-Kendall test was used to evaluate possible trends directly in the peak annual flow data. The trend test was applied to both the magnitude of peak annual flows over time as well as the timing (month) of peak annual flows. As in the previous section, periods of interest included all data from 1947-1998, early period (1947-1980), late period (1981-1998), PDO- (1947-1976), and PDO+ (1977-1998).

2.3 Detection limits for known trends

Regardless of whether climate change or climate variability effects can be detected in the current available flow records, it is instructive to know what the limits of detection may be given a set of known flow trends. In order to do so, a Monte Carlo technique was used to generate many samples of peak annual flow data with prescribed trends. The simulated peak annual flow series were generated such that the de-trended data were drawn from a Log-Pearson III distribution with specified log-mean, log-standard

deviation, and skew coefficients. The steps used to generate the random sequences are included in Appendix A.

The general approach was as follows. Peak annual series for 20 to 100 years were generated and split into two samples (early and late period) for the purpose of testing for statistically significant differences between the samples. For each simulation, the early period sample (S1) was used with PeakFQ to estimate the flood distribution/quantiles as well as the 95% confidence interval for each quantile. Quantile estimates from the later period (S2) were then compared with the confidence intervals from S1. If the later period quantile estimate was outside of the confidence limit from the early period then the difference (trend) was said to be detected.

This analysis was conducted for all combinations of the following parameters:

Log-Pearson III Parameters (based on flow at station)
Low log-C.V.*/ Low log-skew** (Shakespeare)
Low log-C.V./High log-skew (Kenai)
High log-C.V./Low log-skew (Beaver)
High log-C.V./High log-skew (Ninilchik)
*log-C.V. is the coefficient of variation (standard deviation ÷ mean) of the log transformed peak annual flows
**log-skew is the skew coefficient for the flow logarithms

Trend Magnitude
+2.50% of historical average peak annual flow
+1.00%
+0.50%
-0.10%
-0.25%
-0.50%
-1.00%

Sample Size (Years of Record)
20 years (*n1* = *n2* = 10 years)*
40 years (*n1* = *n2* = 20 years)
60 years (*n1* = *n2* = 30 years)
80 years (*n1* = *n2* = 40 years)
100 years (*n1* = *n2* = 50 years)
*With a total of *n* years of data, two samples of *n/2* can be formed

The results were summarized in a table indicating how many years of record would be required to reliably detect trends of known magnitude.

2.4 Confidence intervals for flood risk

Following Bulletin 17B formulae, PeakFQ outputs estimates of specific flood quantiles (flow rates with specified return periods) as well as upper and lower confidence limits for each estimate. Another way of viewing the same data is to specify a flow rate and provide an estimate of the probability of exceedence (return period). The standard output frequency curves (flow versus probability of exceedence) were used with linear interpolation between tabulated points on each curve to derive the confidence limits for probabilities of exceedence (risk) rather than flow rates.

2.5 Site Selection

Annual peak flow records were obtained from the US Geological Survey (USGS) for 70 stream gaging sites in Southcentral Alaska. These sites were screened for general suitability to climate change detection analysis. Criteria used to select sites for further analysis included: length and completeness of record (at least 20 years of systematic record and at least 7 years of data in each of the split-sample periods), absence of in-stream obstructions such as dams, and stations not affected by events such as glacier-dam breaks. Twelve stations were selected for this study and are shown on the map in Figure 1. Site characteristics are listed in Table 1.

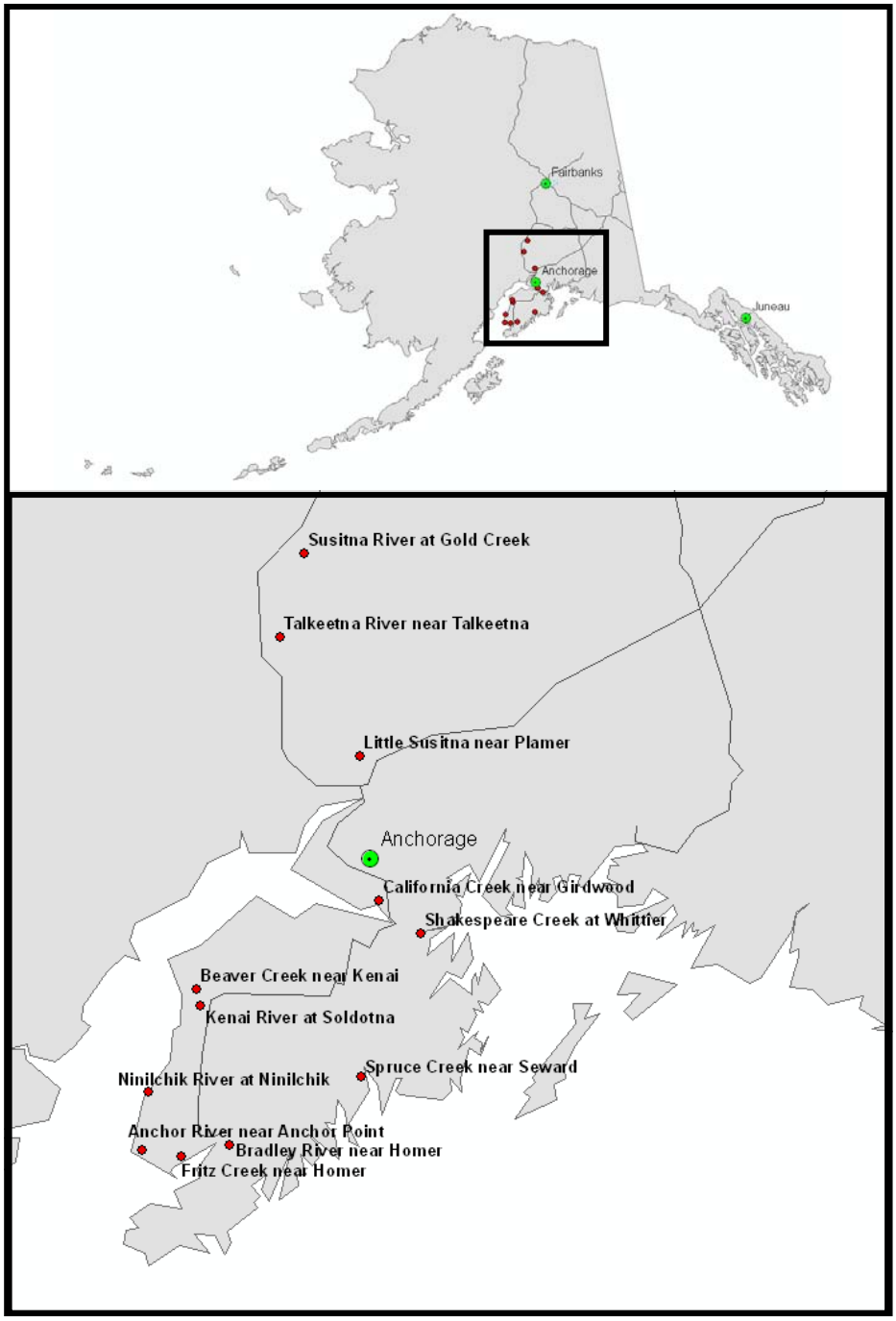

Figure 1: Study site location map.

Table 1: Study site characteristics.

Site Name/ID	Systematic Record Length (years)	Average Peak Annual Flow (cfs)	Drainage Area (mi^2)	Glaciers (%)
15290000 Little Susitna near Palmer	59	2169	61.9	5
15292000 Susitna River at Gold Creek	53	47894	6160	5
15239500 Fritz Creek near Homer	45	172	10.4	0
15266300 Kenai River at Soldotna	43	20047	1951	11
15292700 Talkeetna River near Talkeetna	43	28914	1996	7
15238600 Spruce Creek near Seward	42	2063	9.3	8
15236200 Shakespeare Creek at Whittier	35	455	1.6	50
15239000 Bradley River near Homer	33	3267	56.1	36
15241600 Ninilchik River at Ninilchik	28	845	135	0
15239900 Anchor River near Anchor Point	27	2123	137	0
15272530 California Creek near Girdwood	26	234	7.2	4
15266500 Beaver Creek near Kenai	25	245	51	0

Chapter 3: Results

3.1 Split sample tests for changes in flood quantiles

The analyses reported in this and the following section focused on identifying evidence in the observational record that indicates climate variability and change may be influencing peak annual flows. The first approach, as discussed previously, was to use split sample hypothesis tests to determine if statistically significant changes have occurred over time in the annual flood distributions (i.e., distribution parameters and quantiles of interest). The second approach was to look for trends in the annual maximum flow series directly.

Given the limited extend of observational data in Alaska, only one full cycle of the PDO can be analyzed. As a result, the early period of record tends to overlap considerably with the negative PDO phase (PDO-), while the late period of record overlaps with the positive PDO phase (PDO+). Even so, the full period of record was split in two ways to maximize sample sizes for each of the two hypothesis tests that were conducted. The details of each hypothesis test and years considered in the analysis are as follows:

Test A

Null Hypothesis (Ho): Flood quantiles (flood frequency estimates) have no time-dependent trend.

Alternate Hypothesis (Ha): Flood quantiles are changing over time.

Early period: years 1980 and earlier
Late period: years 1981 and later

Test B

Null Hypothesis (Ho): Flood frequency estimates are independent of PDO phase.

Alternate Hypothesis (Ha): Flood frequency estimates are preconditioned on the phase of the PDO.

PDO- period: years 1947-1976 (Note: no station records before 1949 were used)
PDO+ period: years 1977-1998

As an example of the output for each station, the flood frequency curves for the Early and Late periods at Susitna River at Gold Creek are shown in Figure 2. The x-axis represents a flow probability of exceedence, which is the probability that a given flow rate (y-axis) will be exceeded in any given year. The frequency curve for each sample period (Early or Late) is accompanied by a 95% confidence interval (CI), as generated from PeakFQ. (Note that the bootstrapped CIs were compared with those generated from PeakFQ and found to be consistent.) In this example it is seen that flood frequency estimates for very high flows are significantly different across the two periods of record, while low flow estimates are nearly indistinguishable. Frequency curves for each station and test are presented in Appendix B.

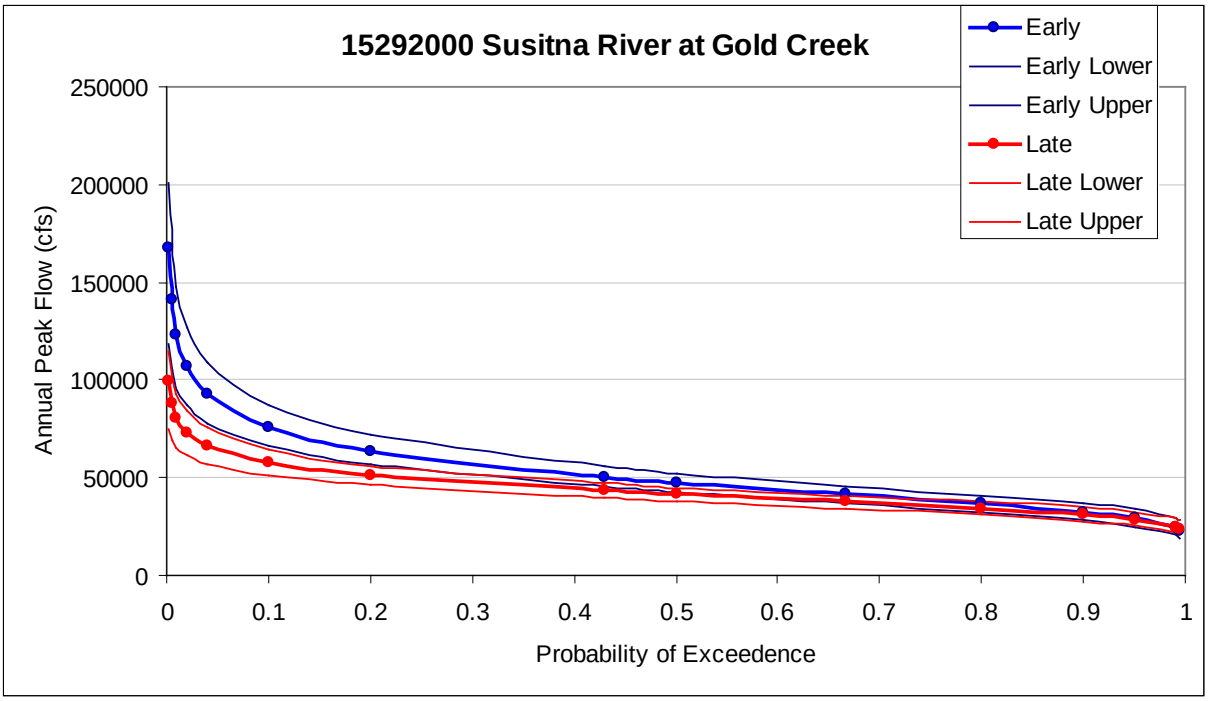

Figure 2: Comparison of estimated flood quantiles for Susitna River at Gold Creek. Estimates for the early period (prior to 1981) are shown in blue, while late period (1981 and later) are shown in red. Bold lines represent the expected value of the quantile, while thin lines show upper and lower limits for 95% confidence intervals.

The bootstrap-generated results for hypothesis tests A and B are summarized in Tables 2 and 3 below. The bootstrap procedure enables tabulation of the actual p-values

associated with differences between Sample 1 and Sample 2 as compared to the null distribution (see section 2.1).

Table 2: Statistical test results for Hypothesis Test A. *n_1 and n_2 represent sample sizes within the early (prior to 1981) and late (1981 and later) periods, respectively. Results represent the p-value for each test, where a value below 0.05 (green highlighting) indicates a significant increase in the flood event over time at the 5% confidence level; a value above 0.95 (yellow highlighting) indicates a significant decrease in the flood event over time at the 5% confidence level.*

		Sample Size		P-Values								
Station ID	**Early vs Late**	**n_1**	**n_2**	**Q 1-yr**	**Q 2-yr**	**Q 5-yr**	**Q 10-yr**	**Q 25-yr**	**Q 50-yr**	**Q 100-yr**	**Q 200-yr**	**Q 500-yr**
15290000	Little Susitna near Plamer	32	27	0.795	0.873	0.847	0.814	0.786	0.774	0.761	0.750	0.737
15292000	Susitna River at Gold Creek	31	22	0.412	0.949	0.985	0.985	0.981	0.977	0.973	0.969	0.961
15239500	Fritz Creek near Homer	18	27	0.037	0.060	0.171	0.238	0.267	0.270	0.262	0.241	0.223
15266300	Kenai River at Soldotna	16	27	0.038	0.927	0.894	0.831	0.742	0.691	0.638	0.581	0.532
15292700	Talkeetna River near Talkeetna	17	26	0.914	0.899	0.720	0.624	0.551	0.517	0.488	0.474	0.456
15238600	Spruce Creek near Seward	15	27	0.124	0.186	0.188	0.210	0.227	0.233	0.229	0.226	0.218
15236200	Shakespeare Creek at Whittier	11	24		0.047	0.306	0.569	0.731	0.776	0.797	0.810	0.817
15239000	Bradley River near Homer	23	10	0.521	0.707	0.376	0.229	0.134	0.100	0.079	0.068	0.061
15241600	Ninilchik River at Ninilchik	18	10		0.517	0.192	0.181	0.184	0.192	0.194	0.197	0.199
15239900	Anchor River near Anchor Point	11	16	0.698	0.024	0.033	0.043	0.065	0.077	0.094	0.104	0.116
15272530	California Creek near Girdwood	14	12	0.043	0.879	0.982	0.989	0.985	0.982	0.977	0.970	0.954
15266500	Beaver Creek near Kenai	12	13	0.064	0.131	0.318	0.430	0.540	0.597	0.639	0.670	0.696

Table 3: Statistical test results for Hypothesis Test B. *n_1 and n_2 represent sample sizes within the PDO negative (1947-1976) and PDO positive (1977-1998) periods, respectively.*

		Sample Size		P-Values								
Station ID	**PDO (-) vs (+)**	**n_1**	**n_2**	**Q 1-yr**	**Q 2-yr**	**Q 5-yr**	**Q 10-yr**	**Q 25-yr**	**Q 50-yr**	**Q 100-yr**	**Q 200-yr**	**Q 500-yr**
15290000	Little Susitna near Plamer	28	22	0.919	0.896	0.924	0.916	0.898	0.893	0.886	0.882	0.873
15292000	Susitna River at Gold Creek	27	20	0.842	0.967	0.970	0.967	0.963	0.963	0.965	0.963	0.964
15239500	Fritz Creek near Homer	14	22	0.018	0.083	0.379	0.483	0.541	0.551	0.557	0.553	0.556
15266300	Kenai River at Soldotna	12	22	0.061	0.584	0.549	0.511	0.450	0.412	0.376	0.350	0.319
15292700	Talkeetna River near Talkeetna	13	22	0.824	0.845	0.746	0.706	0.676	0.658	0.648	0.646	0.646
15238600	Spruce Creek near Seward	11	22	0.098	0.156	0.232	0.271	0.296	0.301	0.306	0.306	0.304
15236200	Shakespeare Creek at Whittier	7	19		0.010	0.040	0.114	0.263	0.349	0.402	0.438	0.473
15239000	Bradley River near Homer	19	14	0.416	0.217	0.111	0.086	0.069	0.067	0.073	0.075	0.082
15241600	Ninilchik River at Ninilchik	14	9		0.444	0.554	0.622	0.686	0.710	0.730	0.739	0.751
15239900	Anchor River near Anchor Point	9	10	0.739	0.024	0.037	0.051	0.075	0.088	0.096	0.113	0.143
15272530	California Creek near Girdwood	10	16	0.006	0.787	0.985	0.995	0.996	0.995	0.994	0.993	0.984
15266500	Beaver Creek near Kenai	9	16	0.046	0.047	0.181	0.297	0.476	0.585	0.669	0.726	0.772

As can be seen in the tables above, the results of Hypothesis Tests A and B are generally in agreement as would be expected due to the substantial overlap of sample periods. Two stations (Susitna at Gold Cr. and California Cr.) indicate decreasing peak flows over a large range of return periods, though generally with respect to more of the quantiles above the distribution average. On the other hand, several stations indicate significant increases on the lower end of the flood distribution (flows exceeded on average every 1 to 2 years). As will be shown later (section 3.3), the power of the statistical tests to detect changes decreases at the high end of the distribution (high return period flows).

In an attempt to gain more insight into the role of climate change, stations with sufficient records were further analyzed for possible time trends within a given phase of the PDO. Five stations had sufficient data to support a test of early versus late flood frequencies

occurring entirely within the PDO negative phase; three of the five stations exhibit a statistically significant trend. Note, in all cases a minimum sample size was set at 7 years of data. This is also the minimum number of years that the USGS considers for flood frequency analysis in Alaska (Curran et al., 2003). Ten stations could support a test of early versus late flood frequencies occurring entirely within the PDO positive phase; four of the ten stations exhibit a statistically significant trend. The findings from these additional tests suggest that for stations showing within-phase trends, flood values generally appear to increase with time during the PDO- phase and decrease with time during the PDO+ phase. Even for stations with an overall decreasing trend on a longer time scale (e.g., Susitna River @ Gold Creek 1947-1998), analysis of the PDO- (early) period shows an increasing trend for the shorter period (1947-1976). This result suggests that climate variability is an important factor in decadal to multi-decadal scale flood frequency changes.

3.2 Test for trends in magnitude and timing of annual maximum flow

The previous section addressed possible trends in derived flood distributions. Trends in the underlying annual maximum flow series are considered in this section. Two types of trends were investigated: 1) trends in the magnitude of peak annual flows, and 2) trends in the timing of peak annual flows. The test used in each case was the nonparametric Mann-Kendall test for the presence of trends. Results are reported for three time periods: PDO- (1949-1976), PDO+ (1977-1998), and the period bounding both phases of the PDO (1949-1998). The purpose of these separate periods is to compare the presence or absence of trends *within* a particular mode of the PDO with those that may exist over a longer study period. Results are summarized in Table 4.

Table 4: Results of the Mann-Kendall test for trends in the magnitude and timing of peak annual floods. Only statistically significant trends are noted (+ significant at the 10% level, * significant at the 5% level) followed by the trend direction (positive/negative).

	Peak Magnitude			Month of peak		
Site Name/ID	**PDO (-)**	**PDO (+)**	**1949-1998**	**PDO (-)**	**PDO (+)**	**1949-1998**
15290000 Little Susitna near Palmer			+ (neg)			
15292000 Susitna River at Gold Creek			+ (neg)			
15239500 Fritz Creek near Homer		+ (neg)				+ (neg)
15266300 Kenai River at Soldotna						
15292700 Talkeetna River near Talkeetna		+ (neg)	* (neg)			
15238600 Spruce Creek near Seward						
15236200 Shakespeare Creek at Whittier						
15239000 Bradley River near Homer						
15241600 Ninilchik River at Ninilchik						
15239900 Anchor River near Anchor Point			+ (pos)			
15272530 California Creek near Girdwood					* (neg)	
15266500 Beaver Creek near Kenai			+ (pos)			

Histograms of the timing (month) of peak annual floods for each station were constructed to aide in a qualitative review of the possible flood-generating mechanisms contributing to each station's peak annual flow records. Three basic patterns were observed among the study sites: a) unimodal distribution with the majority of annual peaks occurring in late summer or fall; b) bimodal distribution with significant spring and summer/fall events; and c) mixed distribution with neither spring nor summer/fall dominating annual peaks. Examples of each pattern are shown in Figure 3.

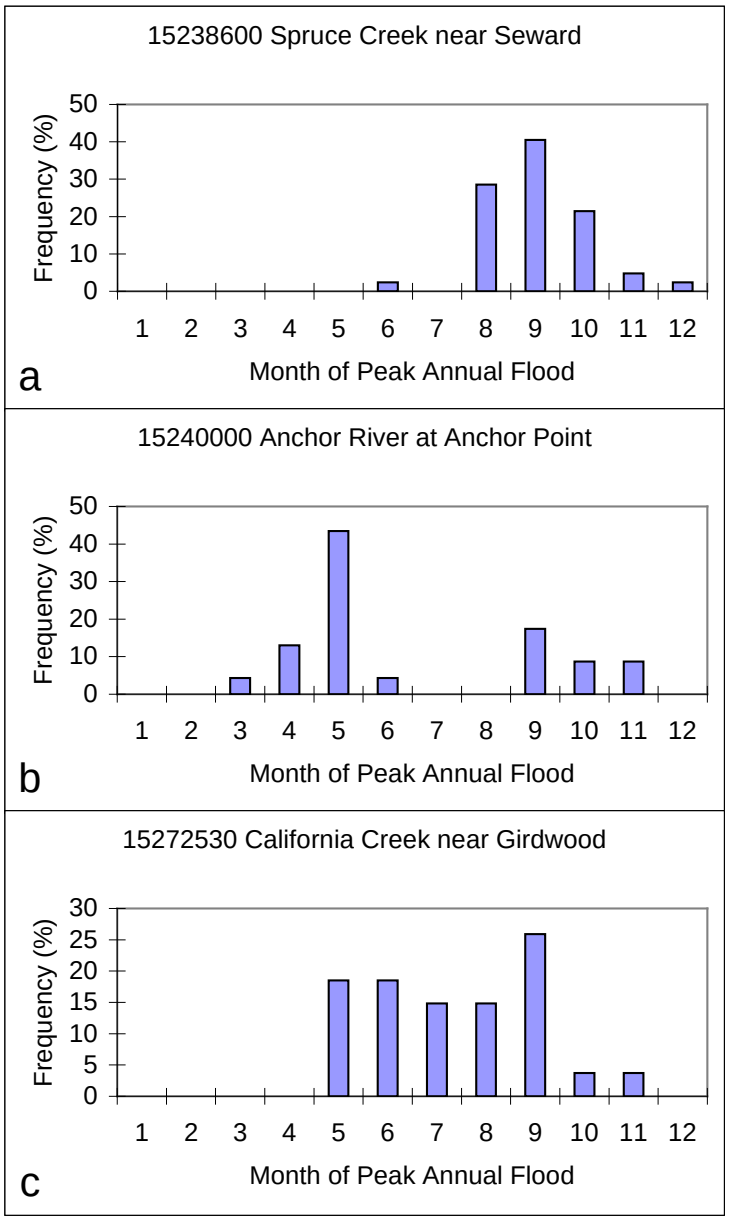

Figure 3: Examples of seasonal distribution of peak annual floods. a) Unimodal distribution dominated by fall rainfall; b) Bimodal distribution with significant spring and fall occurrences; c) Mixed distribution with no single dominate season.

3.3 Detection limits for known trends

The historical data have been reviewed for evidence of climate variability and climate trend influences. However, given the limited observational record and underlying variability of natural systems, it is always possible that existing trends are not yet statistically detectable. The question remains, how much change could take place before it is likely to be detected? Alternatively, for a given rate of change, how many years of record are required to reliably identify emerging biases in our flood frequency estimates?

Following the methods described in section 2.3, a Monte Carlo technique was used to simulate the rate of trend detection for a known trend in the annual maximum flow series and a given length of record available for statistical analysis. Results are presented in Figure 4 for the 2-year and 100-year flood events (exceedence probabilities of 0.5 and 0.01, respectively). For quick reference, detection limits greater than 70% are shaded in either yellow (2-year floods) or green (100-year flood). Simulations were based on four existing Southcentral sites: Shakespeare Creek at Whittier, Kenai River at Soldotna, Beaver Creek near Kenai, and Ninilchik River at Ninilchik. The four stations are representative of the range of annual flood distributions observed in Southcentral Alaska.

Low log-C.V.
Low log-Skew

Imposed Trend (%/Year)		Years of Record Available for Split Sample Testing: 20	40	60	80	100
Increasing Trend	2.50%	55% / 7%	**100%** / 25%	**100%** / 61%	**100%** / **86%**	**100%** / **98%**
	1%	12% / 4%	68% / 7%	**100%** / 19%	**100%** / 43%	**100%** / **70%**
	0.50%	6% / 3%	18% / 3%	67% / 7%	**96%** / 16%	**100%** / 29%
Decreasing Trend	-0.1%	54% / 52%	66% / 54%	65% / 59%	**80%** / 58%	**88%** / 64%
	-0.25%	61% / 55%	**78%** / 61%	**88%** / 68%	**98%** / **75%**	**100%** / **79%**
	-0.5%	69% / 59%	**93%** / 69%	**100%** / **83%**	**100%** / **88%**	**100%** / **94%**
	-1%	**84%** / 64%	**100%** / **84%**	-- / --	-- / --	-- / --

a

* Baseline statistics from Shakespeare Creek at Whittier

Low log-C.V.
High log-Skew

Imposed Trend (%/Year)		Years of Record Available for Split Sample Testing: 20	40	60	80	100
Increasing Trend	2.50%	41% / 10%	**100%** / 23%	**100%** / 41%	**100%** / 62%	**100%** / **82%**
	1%	7% / 6%	52% / 12%	**98%** / 20%	**100%** / 31%	**100%** / 43%
	0.50%	4% / 5%	12% / 9%	54% / 13%	**89%** / 20%	**99%** / 24%
Decreasing Trend	-0.1%	54% / 51%	66% / 51%	65% / 53%	**79%** / 51%	**87%** / 55%
	-0.25%	62% / 53%	**79%** / 55%	**89%** / 57%	**98%** / 58%	**100%** / 62%
	-0.5%	**71%** / 55%	**95%** / 59%	**99%** / 65%	**100%** / 69%	**100%** / **74%**
	-1%	**86%** / 58%	**100%** / 67%	**100%** / **77%**	-- / --	-- / --

b

* Baseline statistics from Kenai River at Soldotna

High log-C.V.
Low log-Skew

Imposed Trend (%/Year)		Years of Record Available for Split Sample Testing: 20	40	60	80	100
Increasing Trend	2.50%	12% / 4%	57% / 4%	**98%** / 8%	**100%** / 13%	**100%** / 21%
	1%	3% / 4%	9% / 2%	34% / 4%	**77%** / 5%	**96%** / 9%
	0.50%	2% / 4%	4% / 2%	10% / 3%	24% / 4%	46% / 5%
Decreasing Trend	-0.1%	51% / 50%	59% / 53%	63% / 54%	66% / 53%	-- / --
	-0.25%	53% / 49%	68% / 53%	**79%** / 53%	-- / --	-- / --
	-0.5%	59% / 50%	-- / --	-- / --	-- / --	-- / --
	-1%	-- / --	-- / --	-- / --	-- / --	-- / --

c

* Baseline statistics from Beaver Creek near Kenai

High log-C.V.
High log-Skew

Imposed Trend (%/Year)		Years of Record Available for Split Sample Testing: 20	40	60	80	100
Increasing Trend	2.50%	14% / 7%	67% / 11%	**99%** / 14%	**100%** / 18%	**100%** / 27%
	1%	3% / 6%	11% / 7%	44% / 11%	**87%** / 11%	**100%** / 17%
	0.50%	2% / 6%	5% / 5%	11% / 9%	32% / 7%	59% / 12%
Decreasing Trend	-0.1%	50% / 49%	61% / 53%	68% / 55%	70% / 52%	**76%** / 54%
	-0.25%	55% / 49%	**72%** / 53%	**85%** / 54%	**91%** / 53%	-- / --
	-0.5%	62% / 50%	**86%** / 53%	-- / --	-- / --	-- / --
	-1%	**73%** / 49%	-- / --	-- / --	-- / --	-- / --

d

* Baseline statistics from Ninilchik River at Ninilchik

Figure 4: Trend detection rate for 2- and 100-year flood events given a specified trend, sample size, and baseline statistical properties (coefficient of variation and skew). Trends

are defined as a percent of the baseline average annual maximum flood per year. Results for the 2-year flood are located in the top left corner of each cell; those for the 100-year flood are in the lower right corner. Results are displayed for log-Pearson III populations with a) low coefficient of variation (CV)/low skew, b) low CV/high skew, c) high CV/low skew, and d) low CV/low skew.

An example of how to read the information presented in Figure 4 is as follows. For a known peak annual flow trend of 1% per annum at a station such as Shakespeare Creek (i.e., with relatively low coefficient of variation and skew in the log-flow distribution), occurring over an observational record of 40 years, there is a 68% likelihood of detecting a trend in the 2-year flood event and a 7% likelihood of detection for the 100-year flood event. However, given 60 years of record, the same split sample test for changes yields a nearly 100% likelihood for detection in the 2-year event and 19% in the 100-year event.

As can be seen, trend detection is much stronger for the 2-year flood than the 100-year flood. Also, detection levels are strongly influenced by the flow variability at a site as well as the direction of the trend. Because annual maximum flows tend to follow a log transformed distribution, and are modeled as such, trends are more readily apparent with decreasing flows than increasing flows.

3.4 Confidence intervals for flood risk

USGS flood frequency estimation includes flow estimates for a number of return periods along with lower and upper confidence limits (at the 95% confidence level) (Curran et al., 2003). For example, a 100-year flood may be estimated as 8,000 cubic feet per second (cfs), with lower and upper confidence limits of 3,750 and 12,400 cfs, respectively. What this means is that there is 95% confidence that the actual 100-year flood is between 3,700 and 12,400 cfs. Another way to view the same statistical output is to consider the design flood of 8,000 cfs and determine the *exceedence probability (or return period)* confidence interval. That is to say, if a structure is designed to safely convey 8,000 cfs on the basis that the 100-year return period poses an acceptable risk, what are the confidence limits on that risk?

For a known exceedence probability of 0.01 (100-year event), probabilities of having at least one excessive flood event ($Q>Q_{100}$) in *N* years are as shown in Table 5.

Table 5: Flood risk over a given time horizon.

N	P(Q≥Q100 at least once)
10	0.10
50	0.39
100	0.63

For example, if a structure has a 50 year design life and is designed to withstand the 100-year flood, there is a 39% chance that the structure will experience an excessive flood event during the design life. However, this assumes that the 100-year flow is perfectly known.

Confidence limits for the risk of exceeding the 100-year design event ($Q>Q_{design}$) within *N* years were calculated for each of the 12 study sites in this project. Table 6 shows the 95% confidence interval for the probability of having at least one excessive flow event in any given 10-, 50-, or 100-year period. In other words, there is 95% confidence that the true flood risk in a given period is between the lower and upper limits listed.

Table 6: 95% Confidence limits for risk of an excessive flood ($Q>Q_{100}$) in *N* years.

Site Name/ID	N=10 years	N=50 years	N=100 years
15290000 Little Susitna near Palmer	0.03 - 0.18	0.16 - 0.62	0.30 - 0.86
15292000 Susitna River at Gold Creek	0.03 - 0.18	0.15 - 0.63	0.27 - 0.86
15239500 Fritz Creek near Homer	0.02 - 0.38	0.10 - 0.91	<0.18 - 0.99
15266300 Kenai River at Soldotna	0.03 - 0.18	0.14 - 0.62	0.25 - 0.86
15292700 Talkeetna River near Talkeetna	0.03 - 0.18	0.13 - 0.63	0.24 - 0.86
15238600 Spruce Creek near Seward	0.03 - 0.18	0.14 - 0.62	0.26 - 0.86
15236200 Shakespeare Creek at Whittier	0.02 - 0.44	0.10 - 0.94	<0.18 - 0.997
15239000 Bradley River near Homer	0.02 - 0.37	0.10 - 0.90	<0.18 - 0.99
15241600 Ninilchik River at Ninilchik	0.02 - 0.33	0.10 - 0.86	<0.18 - 0.98
15239900 Anchor River near Anchor Point	0.02 - 0.33	0.10 - 0.86	<0.18 - 0.98
15272530 California Creek near Girdwood	0.02 - 0.39	0.10 - 0.91	<0.18 - 0.99
15266500 Beaver Creek near Kenai	0.02 - 0.44	0.10 - 0.95	<0.18 - 0.997

An example of how this table may be interpreted is as follows. Given an estimate of the 100-year flow (Q_{100}) at the Susitna River at Gold Creek, the expected risk of exceeding Q_{100} in a 50-year period is 39% (see Table 5). However, considering the uncertainty in the flood frequency estimation, there is 95% chance that the true risk of flooding in 50 years is as low as 15% or as high as 63% (Table 6).

Chapter 4: Discussion

The primary objective of this study has been to evaluate the potential influence of climate variability and climate trends on flood frequency estimates used for transportation design. Several statistical approaches have been applied to the historical peak annual flow data for this purpose. The role of large scale climate variability has been investigated via the climate mode known as the Pacific Decadal Oscillation, which exhibits negative and positive phases. A common approach to investigating long term climate trend influences is to compare early period data to that from a later period. Historical flow data have been

partitioned by PDO mode as well as early/late period and subjected to statistical hypothesis tests for sample differences.

There are a number of complicating factors related to identifying the effects of climate variability and climate trends in the peak annual flood record. First there is the difficulty of clearly separating the driving factors (large scale variability versus long term trends). In general, the available peak flow records in Southcentral Alaska have data corresponding to only one full cycle of the PDO. Consequently, there is an overlap between the early period record with the negative phase of the PDO and the late period record with the positive phase. Without additional PDO positive and negative episodes available for analysis, it is difficult to determine to what extent a long term climate trend may be interacting with underlying climate variability to either enhance or mask differences in the distribution of peak annual flows over time.

It is notable that the majority of study sites reveal no significant changes in their respective peak annual flow distributions at this time (Tables 2 and 3). Of the statistically significant results, more are evident at the high frequency, lower flow, events than at the low frequency, or higher flow, events. At this time there is no clear pattern between percent basin glaciation and significant changes across flood quantiles, even when the difference in underlying variability and length of record are taken into consideration.

However, Hodgkins (2009) found appreciable streamflow changes across Alaska between positive and negative PDO phases and noted that in many cases the magnitude and direction of the changes appear to be related to basin glaciation. Hodgkins' analysis, however, is more directly comparable to the results reported under section 3.2, where annual maximum flows were tested directly, without the use of flood frequency distributions. The overall results, as shown in Table 4, are inconclusive with respect to an overall pattern of change and also do not correlate with Hodgkins' results for glaciated and non-glaciated annual maximum flow trends. However, those results were reported for stations state-wide. Neal et al. (2002) conducted a study of streamflow in Southeast Alaska under PDO positive and negative phases. In that study, seasonal flows were found to differ significantly between the two climate phases, while average annual flows did not.

Southcentral Alaska floods may be the result of one or more mechanisms, including summer/fall storms (rain events), spring snowmelt, or rain-on-snow events (see Figure 3). Furthermore, some streams are subject to significant runoff contributions from glacier melt. The influence of climate variability or climate trends can manifest in the form of intensifying (or deintensifying) a dominant flood mechanism, shifting the timing of peak annual floods, or by altering the relative frequency with which various flood-generating mechanisms represent the peak annual flood. Results from Neal et al. (2002) and Hodgkins (2009) suggest that the PDO may contribute to both seasonal flow changes as well as manifest differently according to the runoff-generating mechanism (e.g., glacial melt). These factors make it particularly difficult to generalize observed changes in annual maximum flows in the Southcentral region.

The results discussed thus far should not be interpreted to mean that change is not occurring. As shown in section 3.3, given the range of underlying variability and the nature of estimating higher order statistics from limited observational data, it may take decades before trends in flood data can be detected, particularly if change is occurring at the extremes of a distribution (e.g., flows greater than Q_{100}). The results shown in Figure 4 underscore the importance of long-term monitoring at key benchmark sites in order to detect change, regardless of the cause. The simulations conducted here imposed linear trends on the annual maximum flow series. The result is that the mean of the flood frequency distribution is most affected, while the tails are less so. It should be noted that there are many other forms that trends could take, including changes in the distribution variance and/or skew in conjunction with changes in mean. It would only make sense to impose such trends in the simulations if they were first informed by modeling of runoff response to climate change, which is beyond the scope of this project.

Finally, uncertainty and variability are often used interchangeably, and both are relevant to risk management as well as trend detection. Unexplained variability in a system contributes to uncertainty in statistical inferences. Furthermore, when uncertainty increases, our power to detect change decreases. Estimates of uncertainty often accompany analytic outcomes, although they are frequently disregarded. For example, the USGS provides estimates of flood quantiles, such as the 25-year or 100-year flood events. A 95% confidence interval is also provided with the estimates and serves to inform the end user of the probable range of the estimated flood. In practice, the estimate alone is used as the basis for infrastructure design. However, there is generally a 50% chance that the actual flood event will be higher than estimated and a 50% chance that it will be lower. As shown in section 3.4, the additional information provided with flood frequency estimates can be presented in such a way as to interpret the range of risk associated with a flood-based design criterion. One approach to using this information is to set an acceptable risk of excessive flooding over the lifetime of a structure, and use the uncertainty estimates that accompany flood estimation to stay within that risk. For example, if the Q_{100} implies a lifetime flood risk of 39% (see Table 5) then an engineer may seek a flood criteria such that there is a 95% likelihood that the *actual* risk will be less than or equal to 39%. As it turns out, this can be done in a straightforward way by selecting the 95^{th} percentile flow from the Q_{100} estimate rather than the expected value, or mean, Q_{100} estimate. The approach is more conservative, but with a quantitative basis. The conservative nature of this approach may also lend added protection in cases where a site is suspected of undergoing adverse flood frequency trends. By selecting the higher end of the quantile estimate, an engineer may minimize the impact of emerging biases due to a climate signal.

Chapter 5: Conclusions and Recommendations

The impetus for this research was a concern that large flood events in Southcentral Alaska may be occurring at greater than expected rates and that the existing flood frequency estimates may become inaccurate due to climate trends. The results discussed here have shown no evidence of significant increases in the very large flood events. In

fact, of the study sites that indicate statistically significant change, increases are seen in the 1- to 5-year flood events, while decreases are noted in the 5- to 500-year events. Perhaps more importantly, there is no evidence of a broad pattern of change in the station records. Furthermore, as a result of the overlap between early period/PDO- samples and late period/PDO+ samples, the current data do not support conclusions regarding the relative influence of long term climate trends versus changing phases of the PDO on flood frequency estimates over time.

The absence of an overriding pattern of change across the study region does not mean that change is not occurring. Analysis of trend detection in flood frequency estimates has shown that trends are particularly difficult to detect for low frequency flood events, such as the 100-year flood. This is due to the uncertainty associated with estimating rare events. However, it also means that even under the condition of a known trend, estimated flood frequencies may remain within the reported uncertainty bands for several decades.

These findings lead to two important recommendations. First, long term monitoring of key sites should be a priority in order to increase the power of change detection and reduce uncertainty associated with flood frequency estimates. Although current evidence of change is limited, it has been shown that substantial change may occur before trends are detected.

Second, design criteria that utilize flood frequency estimates should incorporate additional information about uncertainty. As discussed previously, the confidence limits provided with flood estimates can be used to develop tables of flood risk whereby design engineers can readily select a flood level that provides a 95% probability of remaining at or below the targeted flood risk. The USGS already provides uncertainty bounds with published flood frequency estimates, and the proposed approach can easily be implemented in tabulated form within a design manual.

References

Chowdhury, J.U., and J.R. Stedinger, 1991. "Confidence Interval for Design Floods with Estimated Skew Coefficient." *Journal of Hydraulic Engineering*, 117(7), pp. 811-831.

Curran, J.H., D.F. Meyer, and G.D. Tasker, 2003. "Estimating the Magnitude and Frequency of Peak Streamflows for Ungaged Sites on Streams in Alaska and Conterminous Basins in Canada." U.S. Geological Survey Water Resources Investigations Report 03-4188, 101 p.

Efron, B., 1982. *The Jackknife, Bootstrap, and Other Resampling Plans.* Monograph 38, Society for Industrial and Applied Mathematics, Philadelphia, Pa.

Efron, B., and R. Tibshirani, 1993. *An Introduction to the Bootstrap.* Chapman & Hall/CRC, New York, 436 pp.

Flynn, K.M., Kirby, W.H., and Hummel, P.R., 2006. "User's manual for program PeakFQ, Annual Flood Frequency Analysis Using Bulletin 17B Guidelines." U.S. Geological Survey Techniques and Methods Book 4, Chapter B4, 42 pgs.

Hodgkins, G.A., 2009. "Streamflow changes in Alaska between the cool phase (1947-1976) and the warm phase (1977-2006) of the Pacific Decadal Oscillation: The influence of glaciers." Water Resources Research, 45, W06502, doi: 10.1020/2008WR007575.

Interagency Advisory Committee on Water Data, 1982. "Guidelines for determining flood flow frequency." Hydrology Subcommittee Bulletin 17B.

Kite, G.W., 1988. *Frequency and Risk Analysis in Hydrology*. Water Resources Publications, Colorado, 257p.

Mantua, N.J. and S.R. Hare, Y. Zhang, J.M. Wallace, and R.C. Francis, 1997. "A Pacific interdecadal climate oscillation with impacts on salmon production." *Bulletin of the American Meteorological Society*, 78, pp. 1069-1079.

Neal, E.G., M.T. Walter, and C. Coffeen, 2002. "Linking the Pacific Decadal Oscillation to seasonal stream discharge patterns in southeast Alaska." *J. Hydrology*, 263, 188-197, doi:10.1016/S0022-1694(02)00058-6.

Appendix A: Statistical Derivations

Random Pearson-III Sequences

Let z_p be a Standard Normal variate and y_p be a Pearson-III variate with cumulative probability p. Then yp can be calculated as:

(1) $$y_p = \bar{y} + K_p S ,$$

where $\bar{y}$ and S are the distribution mean and standard deviation, respectively, and K_p is the frequency factor for the Standard Pearson-III distribution. Frequency factor, K_p, can be estimated as follows (Kite, 1988; Chowdhury and Stedinger, 1991):

(2) $$K_p = z_p + (z_p^2 - 1)\frac{\gamma}{6} + \frac{1}{3}(z_p^3 - 6z_p)(\frac{\gamma}{6})^2 - (z_p^2 - 1)(\frac{\gamma}{6})^3 + z_p(\frac{\gamma}{6})^4 + \frac{1}{3}(\frac{\gamma}{6})^5,$$

where γ is the distribution skew and z_p is as previously defined. Thus, a random sequence of Pearson-III variables can be derived from a random sequence of Standard Normal variables, given a specified mean, standard deviation, and skew coefficient.

Random Flows from the Log-Pearson III Distribution

If a variable, X, is distributed as Log-Pearson III, then the logarithms of the variable, $Y=log(X)$, are Pearson III distributed with mean, standard deviation, and skew coefficients $log\text{-}\mu_x$, $log\text{-}\sigma_x$, and $log\text{-}\gamma_x$, respectively. X is calculated from Y as

(3) $$x_i = 10^{y_i} , \; i = 1, 2, \ldots, N.$$

Adding a Linear Trend to Log-Pearson III Sequences

Stationary sequences of Log-Pearson III distributed flows were generated using Equations 1-3 above. A linear trend in the flow data was introduced as follows:

$$x_i' = x_i + \alpha i ,$$

where the sequence index i is interpreted as the year in a time series, and α is a set fraction of the long term average flow (e.g., $\alpha = 0.01\overline{Q}$ for a 1% per annum increasing trend).

Appendix B: Split Sample Results for All Stations

Figures 1-12: Comparison of estimated flood quantiles for each study site. Estimates for the early period (prior to 1981) are shown in blue, while late period (1981 and later) are shown in red. Bold lines represent the expected value of the quantile, while thin lines show upper and lower limits for 95% confidence intervals.

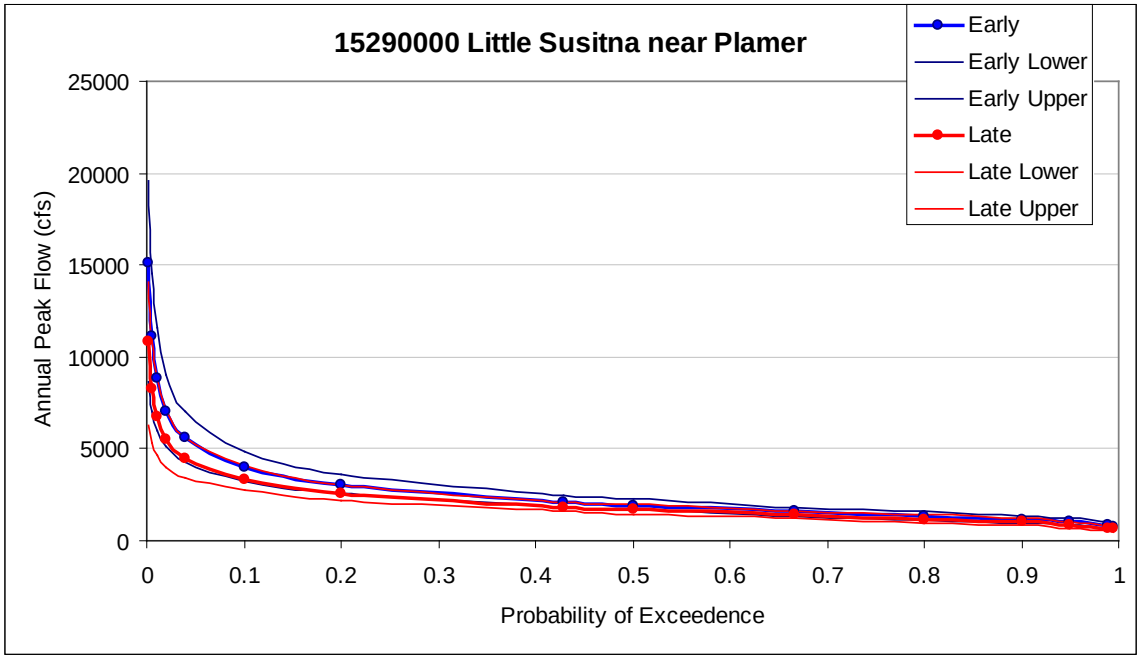

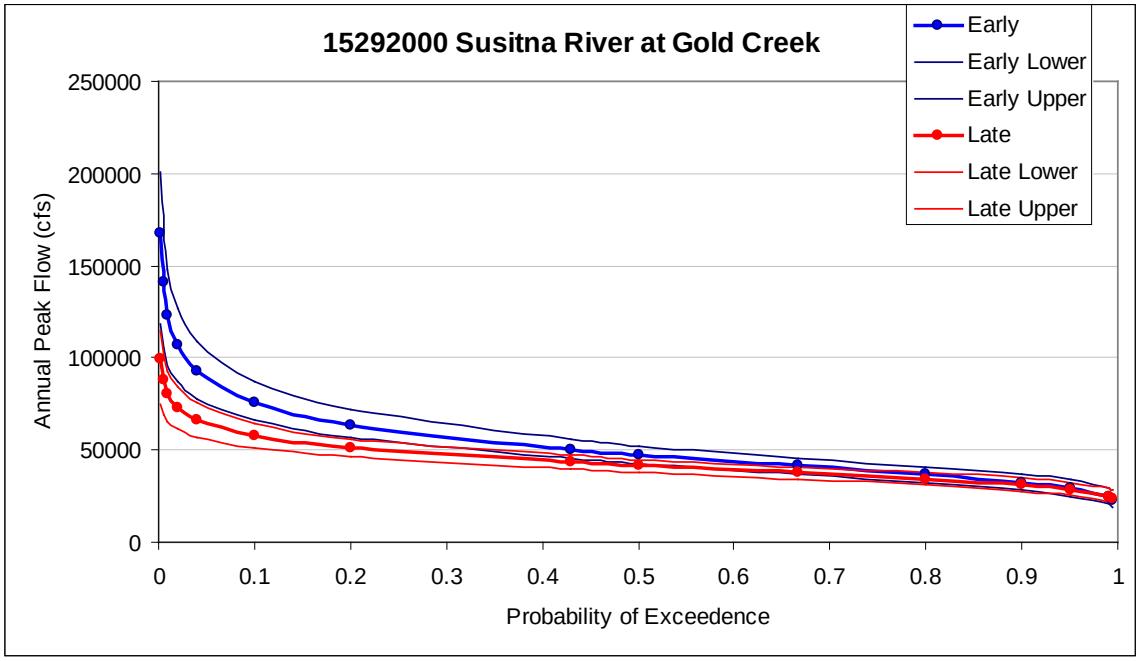

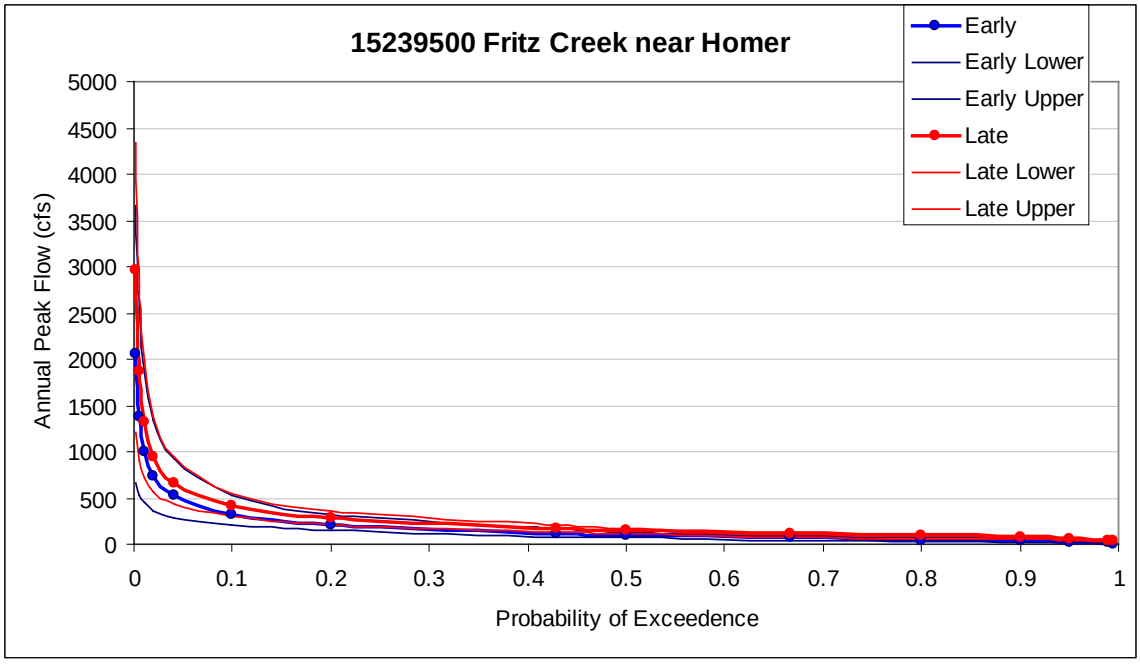
15239500 Fritz Creek near Homer
Early
Early Lower
Early Upper
Late
Late Lower
Late Upper
Annual Peak Flow (cfs)
5000
4500
4000
3500
3000
2500
2000
1500
1000
500
0
0
0.1
0.2
0.3
0.4
0.5
0.6
0.7
0.8
0.9
1
Probability of Exceedence

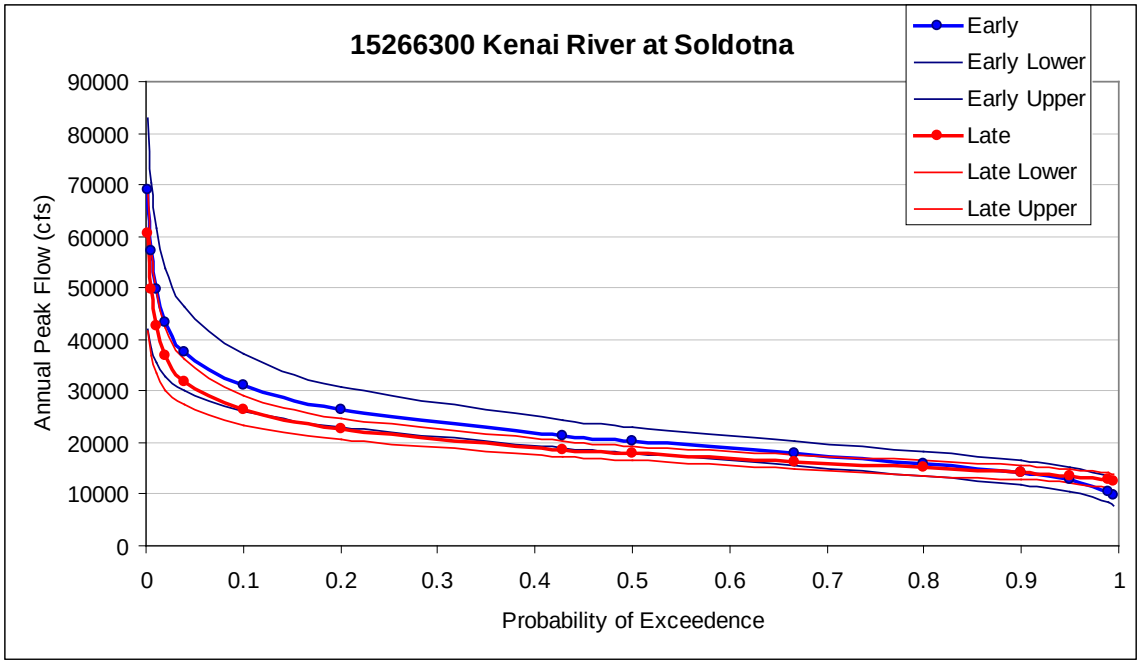
15266300 Kenai River at Soldotna
Early
Early Lower
Early Upper
Late
Late Lower
Late Upper
Annual Peak Flow (cfs)
90000
80000
70000
60000
50000
40000
30000
20000
10000
0
0
0.1
0.2
0.3
0.4
0.5
0.6
0.7
0.8
0.9
1
Probability of Exceedence

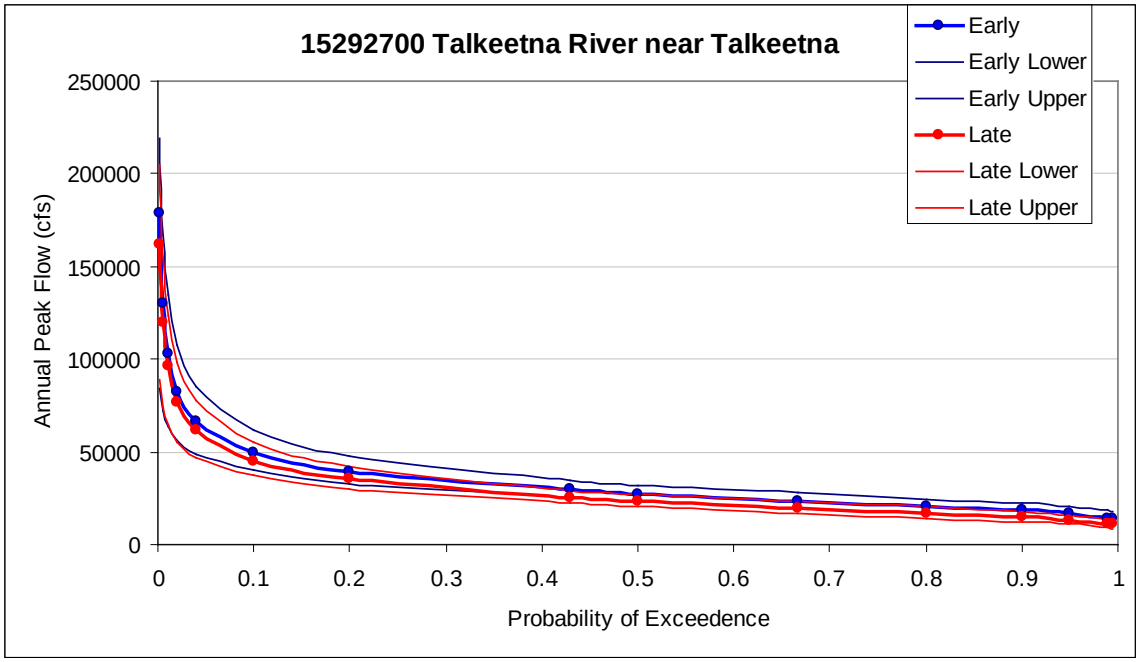
15292700 Talkeetna River near Talkeetna
Annual Peak Flow (cfs)
250000
200000
150000
100000
50000
0
0
0.1
0.2
0.3
0.4
0.5
0.6
0.7
0.8
0.9
1
Probability of Exceedence
Early
Early Lower
Early Upper
Late
Late Lower
Late Upper

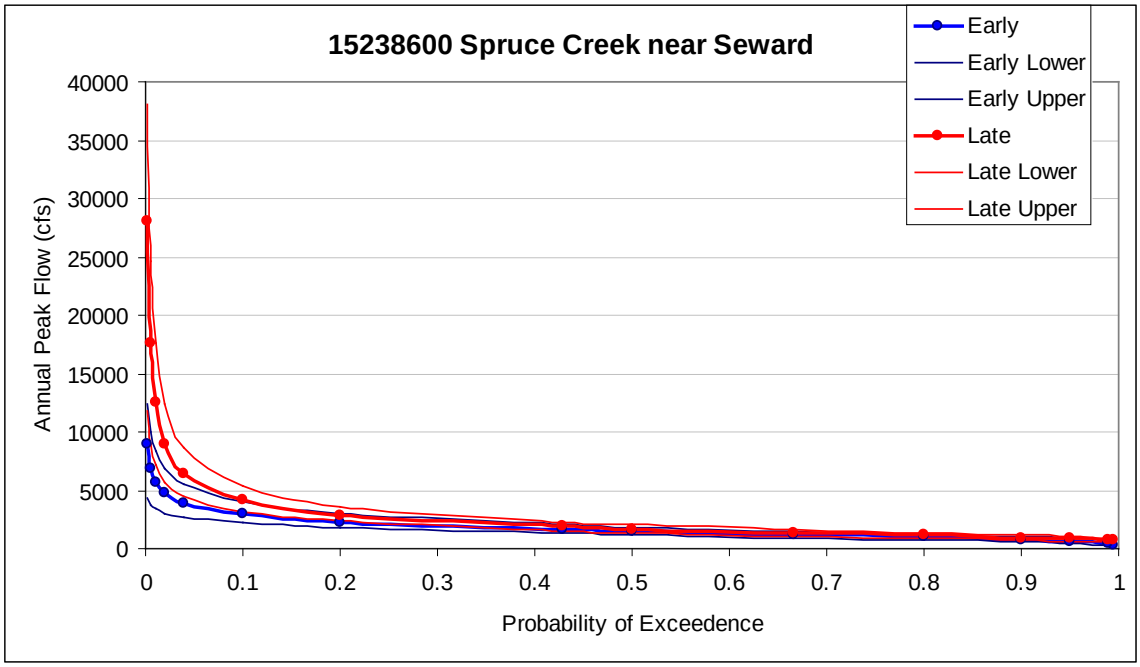
15238600 Spruce Creek near Seward
Annual Peak Flow (cfs)
40000
35000
30000
25000
20000
15000
10000
5000
0
0
0.1
0.2
0.3
0.4
0.5
0.6
0.7
0.8
0.9
1
Probability of Exceedence
Early
Early Lower
Early Upper
Late
Late Lower
Late Upper

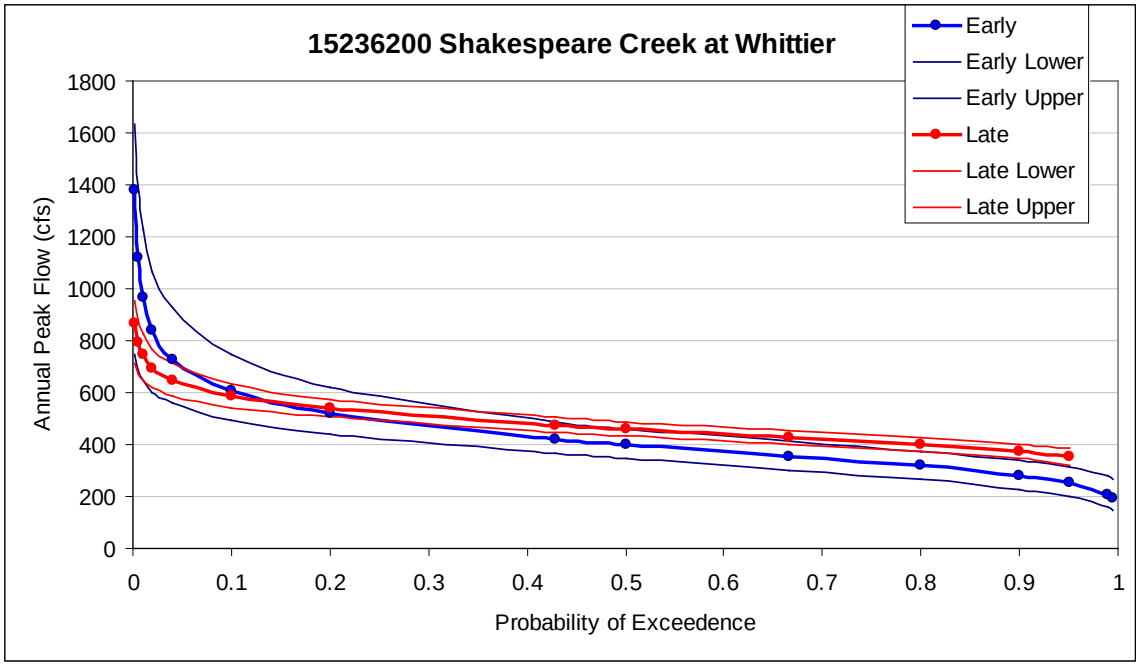
15236200 Shakespeare Creek at Whittier
Early
Early Lower
Early Upper
Late
Late Lower
Late Upper
Annual Peak Flow (cfs)
1800
1600
1400
1200
1000
800
600
400
200
0
0
0.1
0.2
0.3
0.4
0.5
0.6
0.7
0.8
0.9
1
Probability of Exceedence

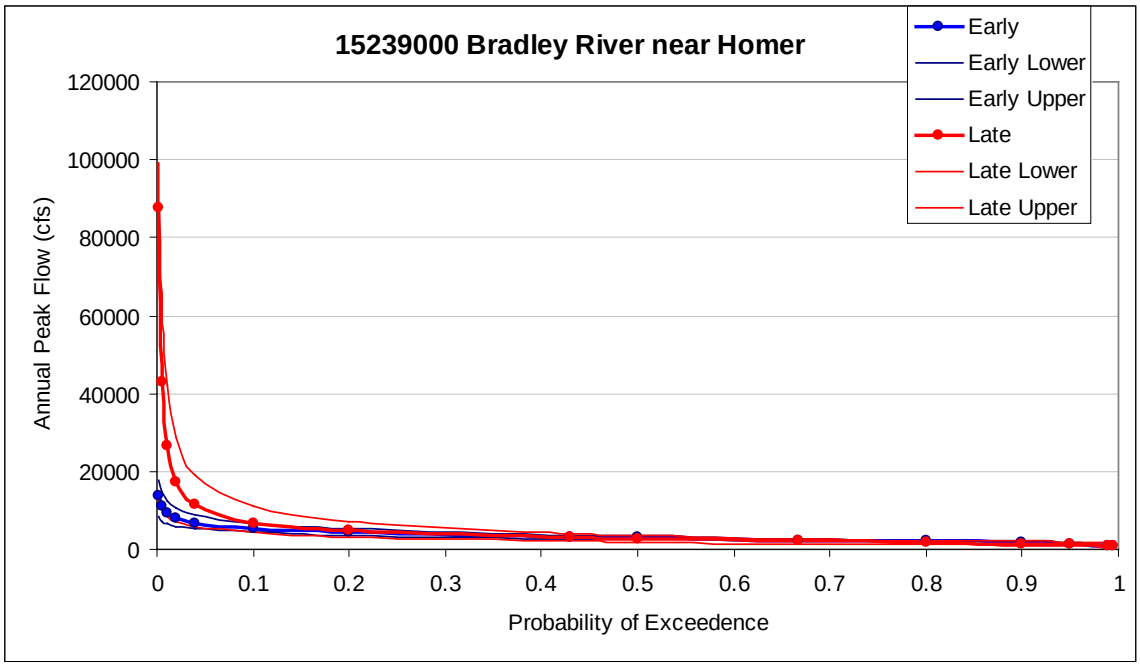
15239000 Bradley River near Homer
Early
Early Lower
Early Upper
Late
Late Lower
Late Upper
Annual Peak Flow (cfs)
120000
100000
80000
60000
40000
20000
0
0
0.1
0.2
0.3
0.4
0.5
0.6
0.7
0.8
0.9
1
Probability of Exceedence

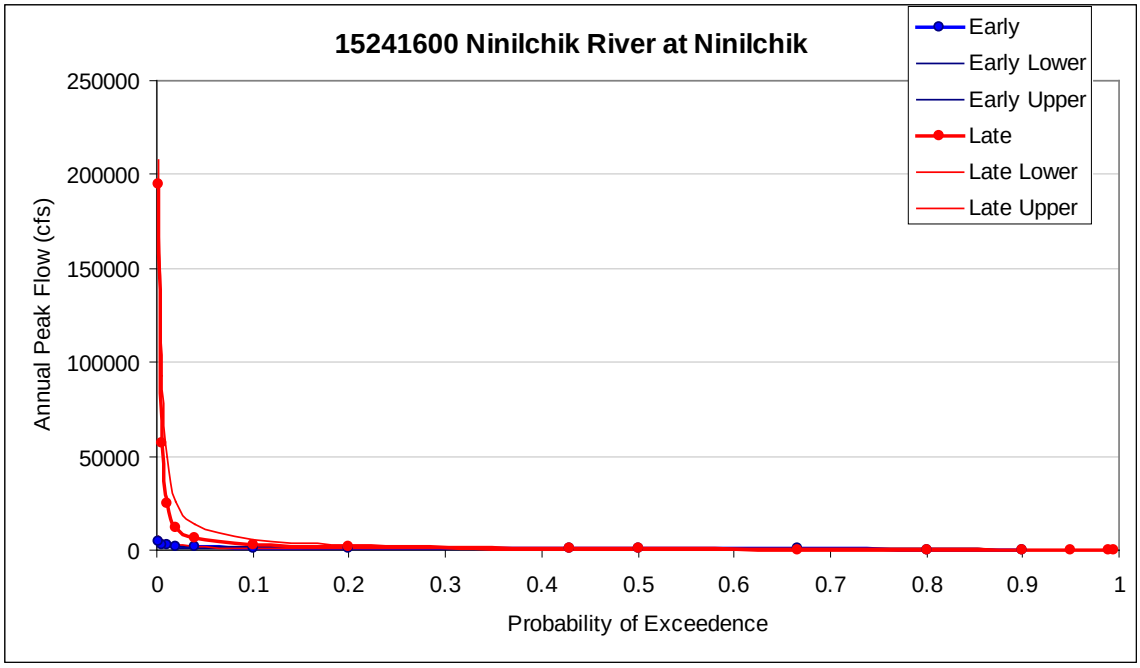
15241600 Ninilchik River at Ninilchik
Early
Early Lower
Early Upper
Late
Late Lower
Late Upper
250000
200000
150000
100000
50000
0
Annual Peak Flow (cfs)
0
0.1
0.2
0.3
0.4
0.5
0.6
0.7
0.8
0.9
1
Probability of Exceedence

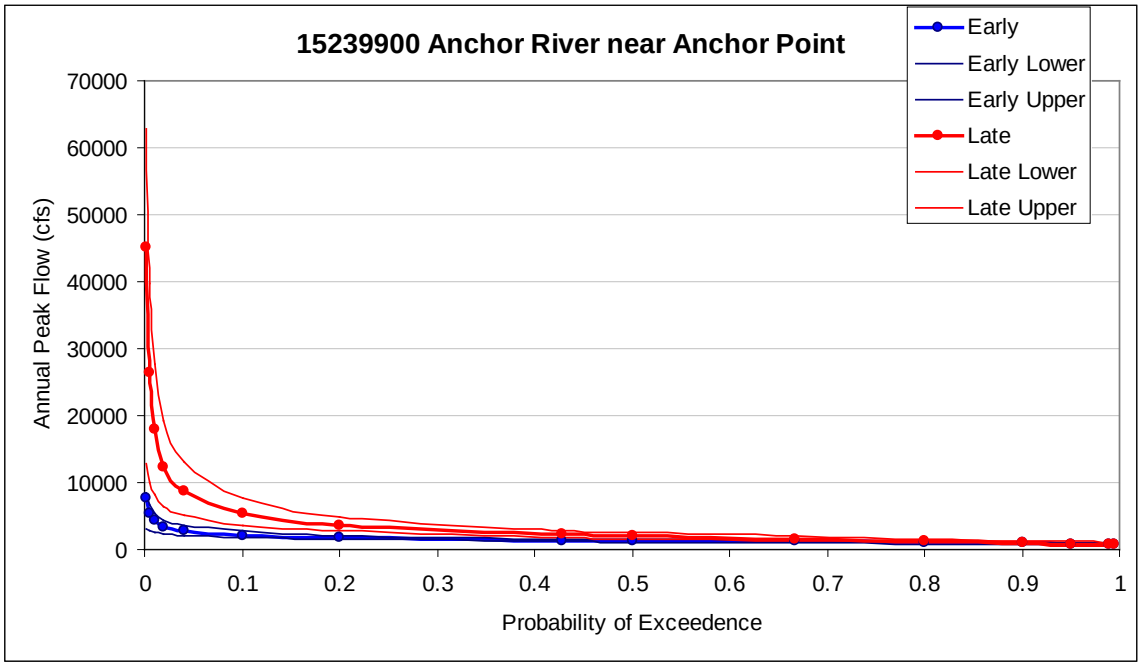
15239900 Anchor River near Anchor Point
Early
Early Lower
Early Upper
Late
Late Lower
Late Upper
70000
60000
50000
40000
30000
20000
10000
0
Annual Peak Flow (cfs)
0
0.1
0.2
0.3
0.4
0.5
0.6
0.7
0.8
0.9
1
Probability of Exceedence

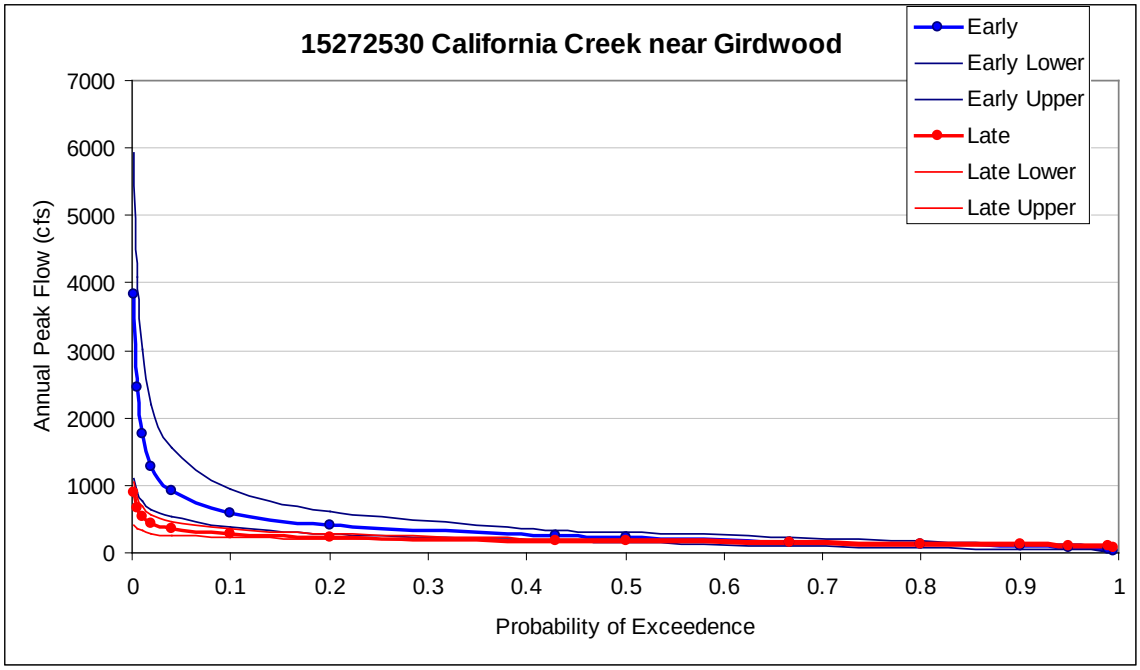
15272530 California Creek near Girdwood
Early
Early Lower
Early Upper
Late
Late Lower
Late Upper
Annual Peak Flow (cfs)
7000
6000
5000
4000
3000
2000
1000
0
0
0.1
0.2
0.3
0.4
0.5
0.6
0.7
0.8
0.9
1
Probability of Exceedence

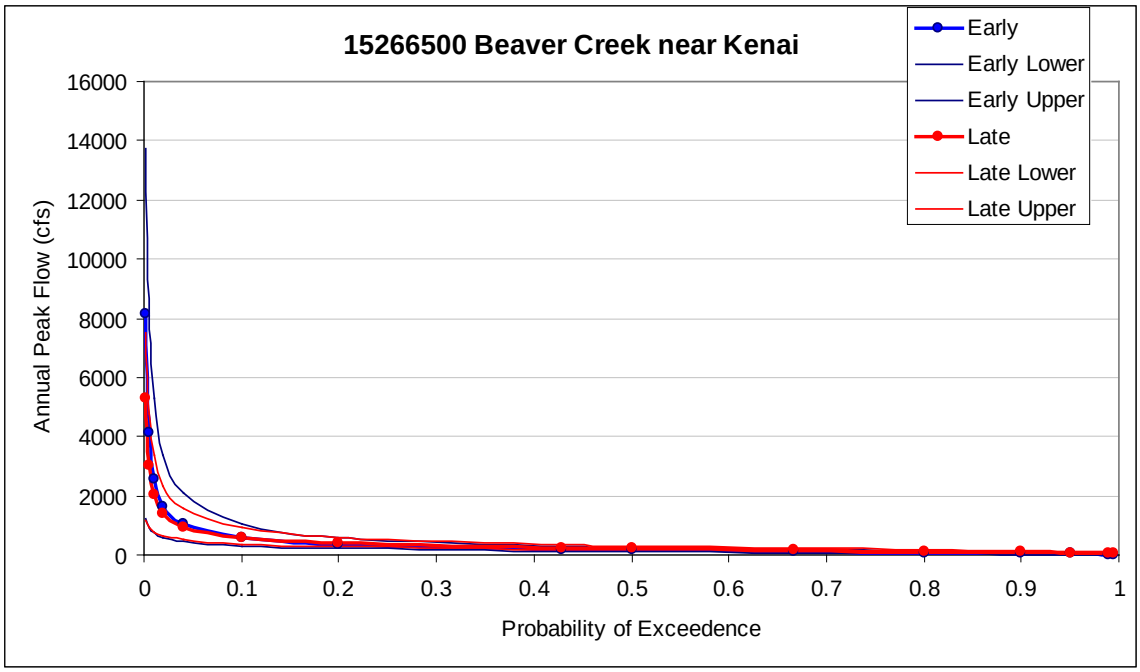
15266500 Beaver Creek near Kenai
Early
Early Lower
Early Upper
Late
Late Lower
Late Upper
Annual Peak Flow (cfs)
16000
14000
12000
10000
8000
6000
4000
2000
0
0
0.1
0.2
0.3
0.4
0.5
0.6
0.7
0.8
0.9
1
Probability of Exceedence

Figures 13-24: Comparison of estimated flood quantiles for each study site. Estimates for the PDO- period (1947-1976) are shown in blue, while PDO+ period (1977-1998) are shown in red. Bold lines represent the expected value of the quantile, while thin lines show upper and lower limits for 95% confidence intervals.

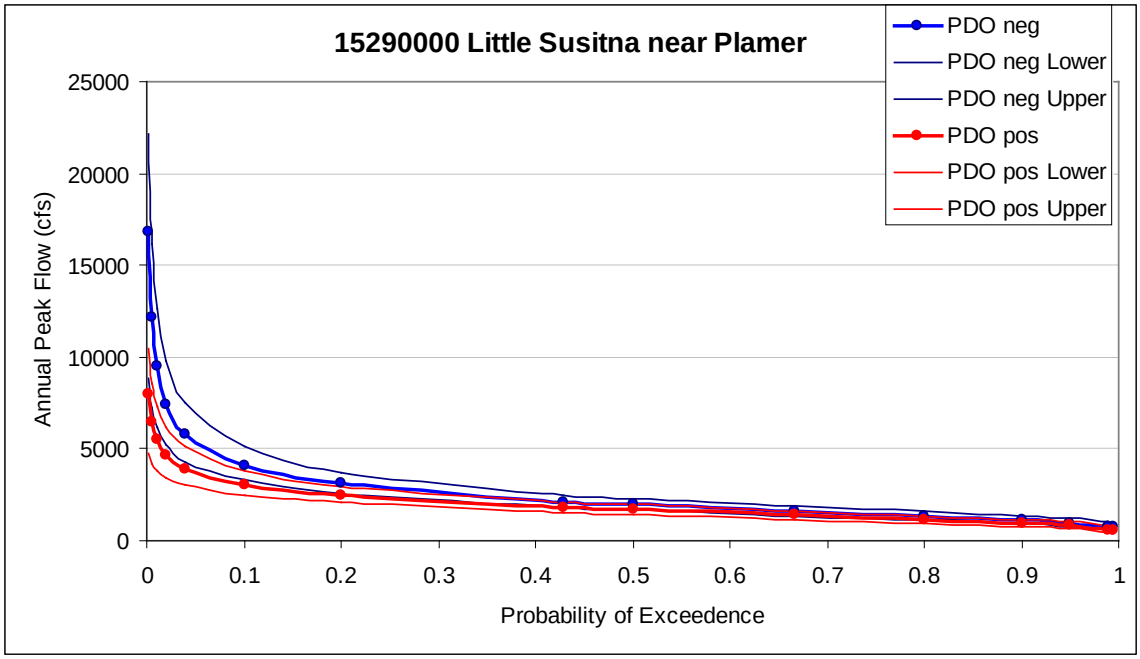

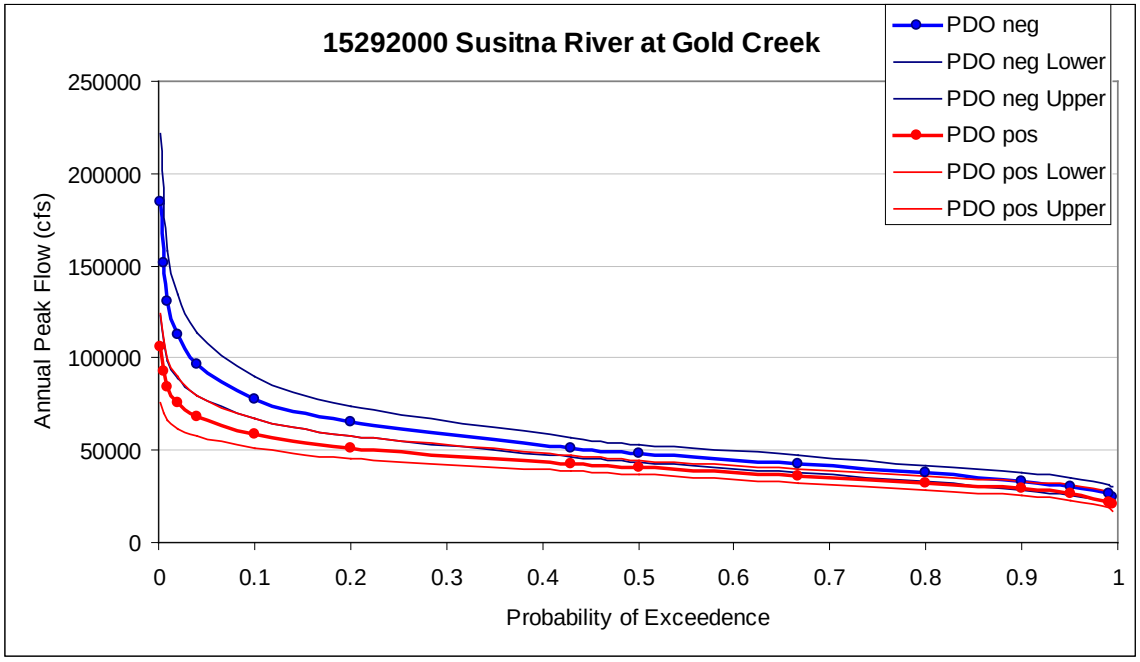

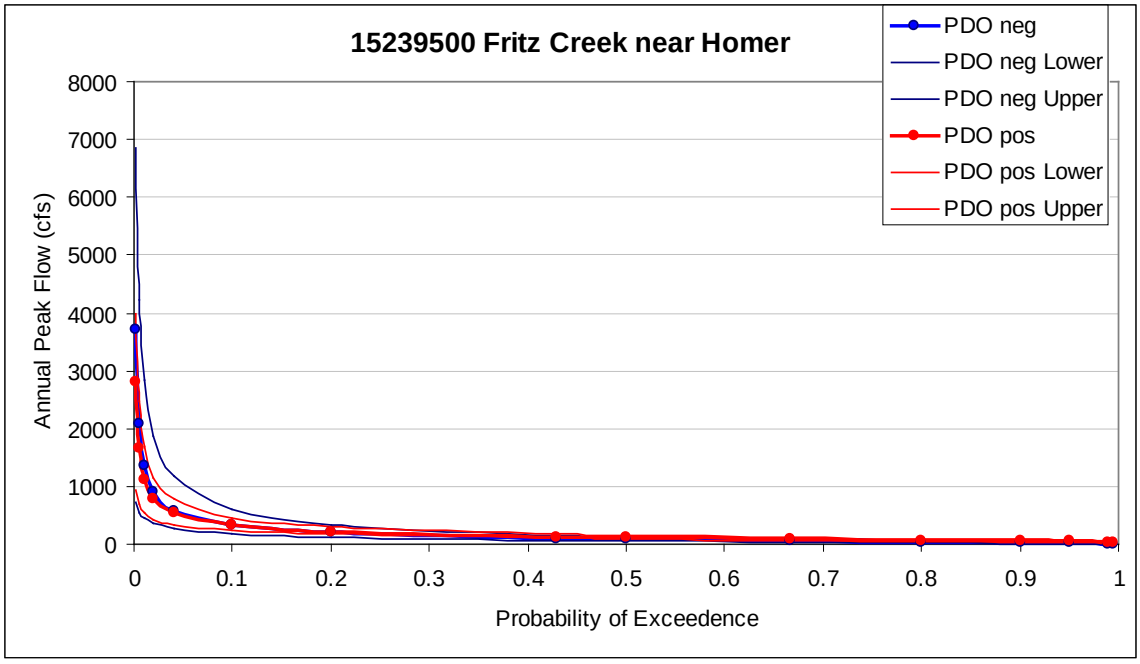
15239500 Fritz Creek near Homer
PDO neg
PDO neg Lower
PDO neg Upper
PDO pos
PDO pos Lower
PDO pos Upper
Annual Peak Flow (cfs)
8000
7000
6000
5000
4000
3000
2000
1000
0
0
0.1
0.2
0.3
0.4
0.5
0.6
0.7
0.8
0.9
1
Probability of Exceedence

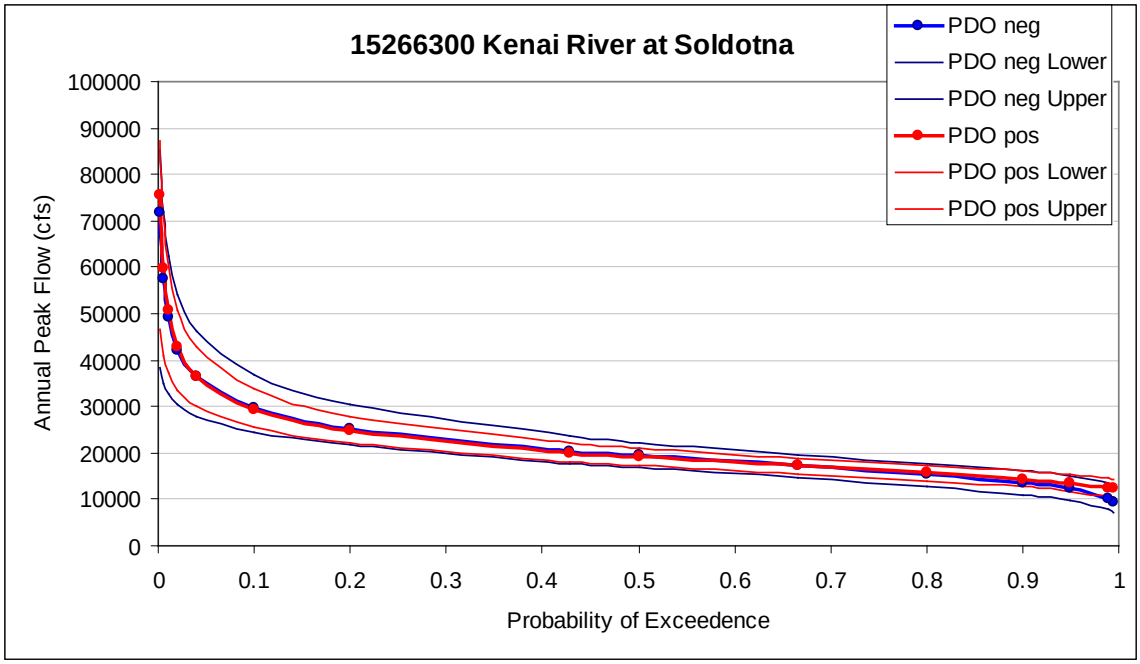
15266300 Kenai River at Soldotna
PDO neg
PDO neg Lower
PDO neg Upper
PDO pos
PDO pos Lower
PDO pos Upper
Annual Peak Flow (cfs)
100000
90000
80000
70000
60000
50000
40000
30000
20000
10000
0
0
0.1
0.2
0.3
0.4
0.5
0.6
0.7
0.8
0.9
1
Probability of Exceedence

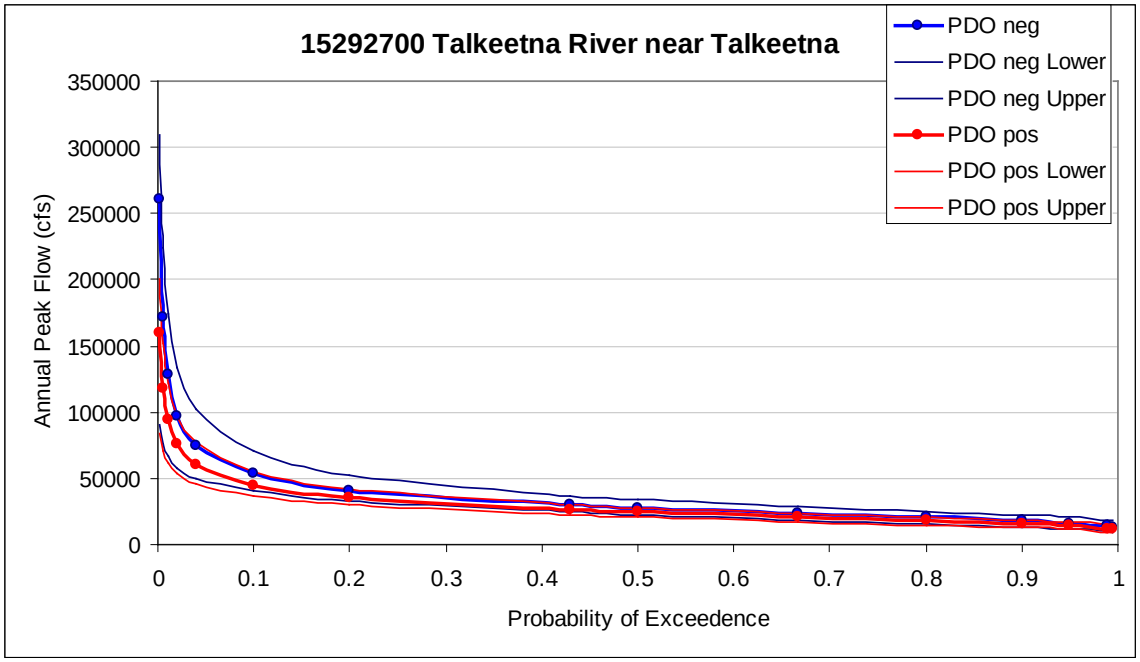
15292700 Talkeetna River near Talkeetna
PDO neg
PDO neg Lower
PDO neg Upper
PDO pos
PDO pos Lower
PDO pos Upper
Annual Peak Flow (cfs)
350000
300000
250000
200000
150000
100000
50000
0
0
0.1
0.2
0.3
0.4
0.5
0.6
0.7
0.8
0.9
1
Probability of Exceedence

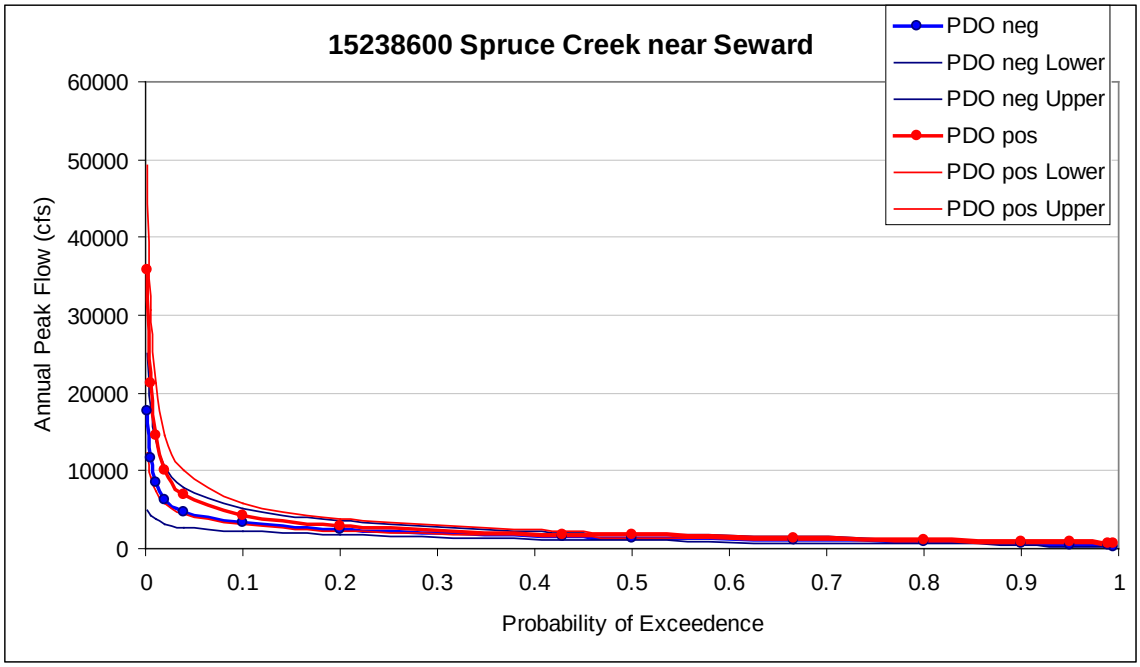
15238600 Spruce Creek near Seward
PDO neg
PDO neg Lower
PDO neg Upper
PDO pos
PDO pos Lower
PDO pos Upper
Annual Peak Flow (cfs)
60000
50000
40000
30000
20000
10000
0
0
0.1
0.2
0.3
0.4
0.5
0.6
0.7
0.8
0.9
1
Probability of Exceedence

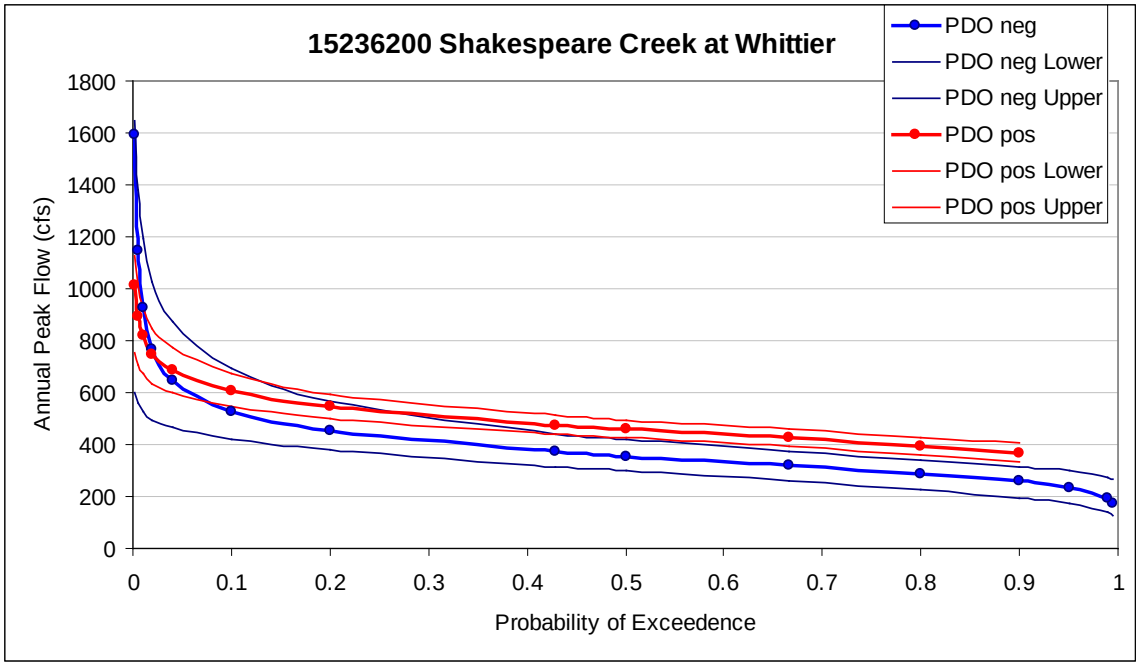
15236200 Shakespeare Creek at Whittier
PDO neg
PDO neg Lower
PDO neg Upper
PDO pos
PDO pos Lower
PDO pos Upper
Annual Peak Flow (cfs)
1800
1600
1400
1200
1000
800
600
400
200
0
0
0.1
0.2
0.3
0.4
0.5
0.6
0.7
0.8
0.9
1
Probability of Exceedence

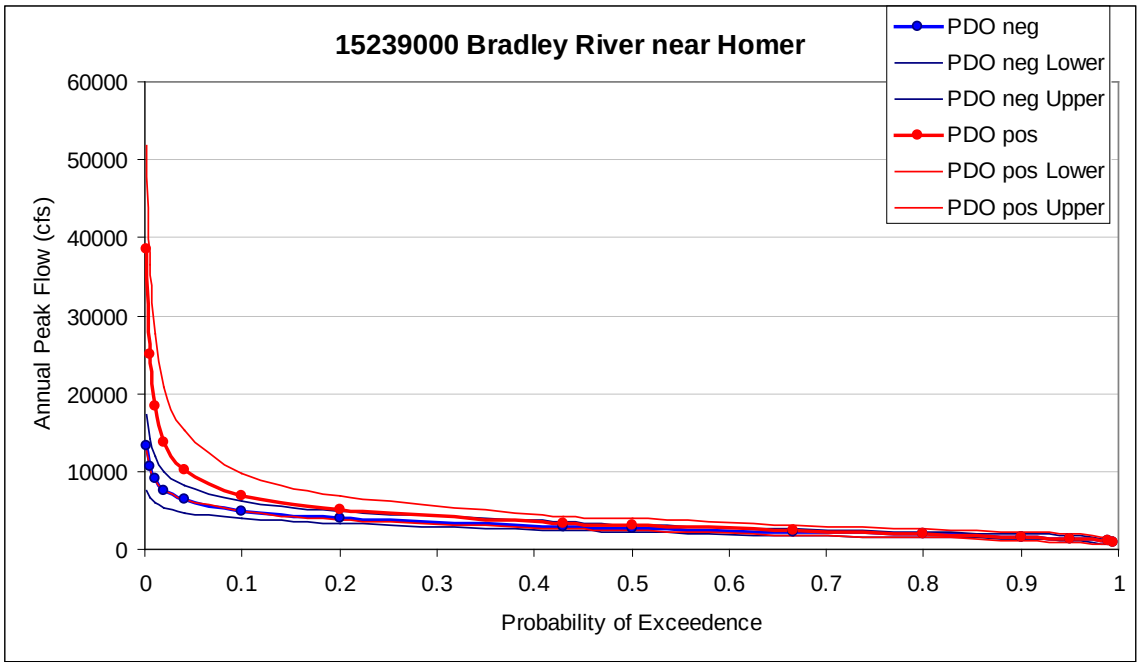
15239000 Bradley River near Homer
PDO neg
PDO neg Lower
PDO neg Upper
PDO pos
PDO pos Lower
PDO pos Upper
Annual Peak Flow (cfs)
60000
50000
40000
30000
20000
10000
0
0
0.1
0.2
0.3
0.4
0.5
0.6
0.7
0.8
0.9
1
Probability of Exceedence

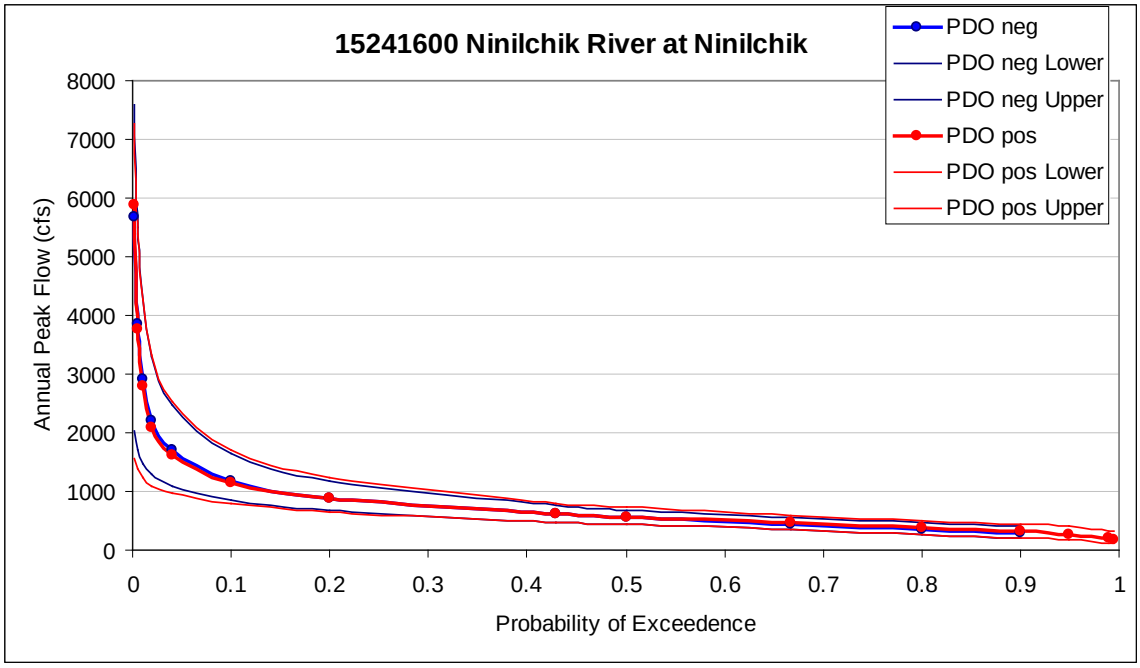
15241600 Ninilchik River at Ninilchik
PDO neg
PDO neg Lower
PDO neg Upper
PDO pos
PDO pos Lower
PDO pos Upper
Annual Peak Flow (cfs)
8000
7000
6000
5000
4000
3000
2000
1000
0
0
0.1
0.2
0.3
0.4
0.5
0.6
0.7
0.8
0.9
1
Probability of Exceedence

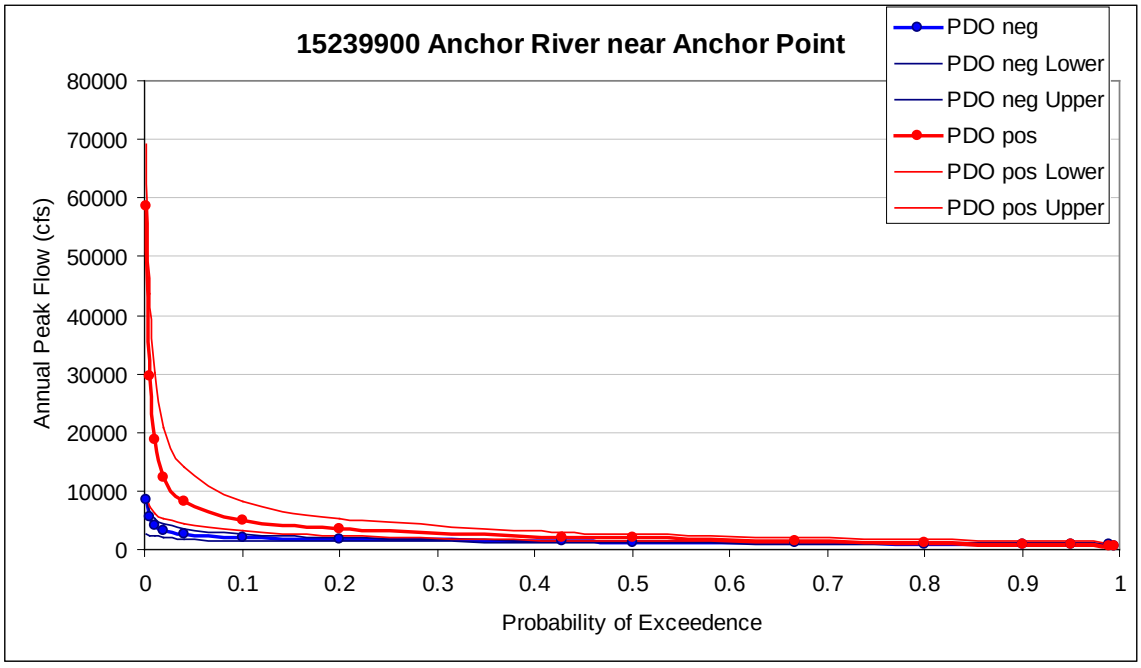
15239900 Anchor River near Anchor Point
PDO neg
PDO neg Lower
PDO neg Upper
PDO pos
PDO pos Lower
PDO pos Upper
Annual Peak Flow (cfs)
80000
70000
60000
50000
40000
30000
20000
10000
0
0
0.1
0.2
0.3
0.4
0.5
0.6
0.7
0.8
0.9
1
Probability of Exceedence

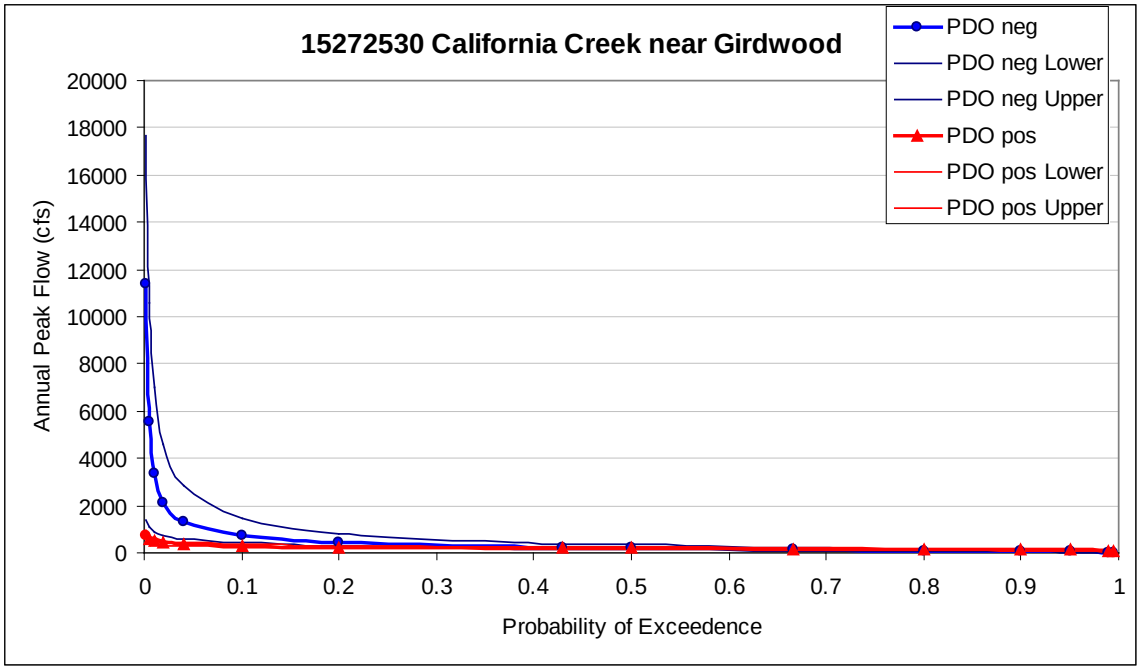
15272530 California Creek near Girdwood
PDO neg
PDO neg Lower
PDO neg Upper
PDO pos
PDO pos Lower
PDO pos Upper
Annual Peak Flow (cfs)
20000
18000
16000
14000
12000
10000
8000
6000
4000
2000
0
0
0.1
0.2
0.3
0.4
0.5
0.6
0.7
0.8
0.9
1
Probability of Exceedence

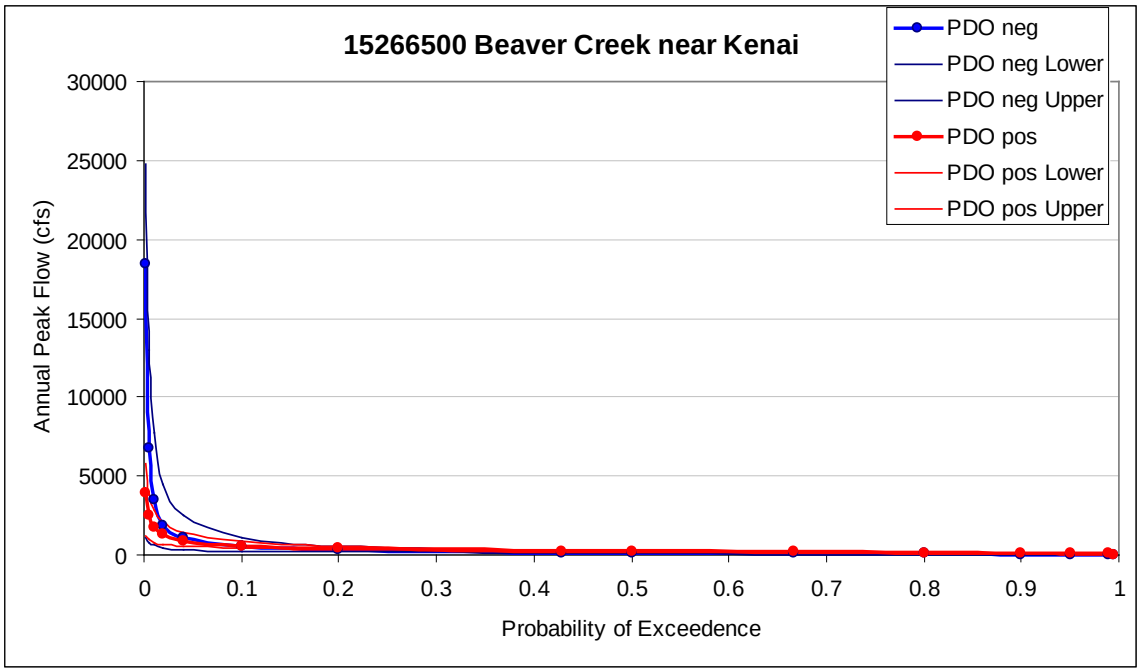
15266500 Beaver Creek near Kenai
PDO neg
PDO neg Lower
PDO neg Upper
PDO pos
PDO pos Lower
PDO pos Upper
Annual Peak Flow (cfs)
30000
25000
20000
15000
10000
5000
0
0
0.1
0.2
0.3
0.4
0.5
0.6
0.7
0.8
0.9
1
Probability of Exceedence